

CORROSION RESISTANT CONCRETE USING CORROSION  
RESISTANT STEEL

by

David Beh

A thesis submitted to the faculty of  
The University of Utah  
in partial fulfillment of the requirements for the degree of

Master of Science

Department of Civil and Environmental Engineering

The University of Utah

August 2013

Copyright © David Beh 2013

All Rights Reserved

**The University of Utah Graduate School**

**STATEMENT OF THESIS APPROVAL**

The thesis of David Beh

has been approved by the following supervisory committee members:

Chris P. Pantelides, Chair 01/16/2013  
Date Approved

Pedro R. Romero, Member 11/19/2012  
Date Approved

Paul J. Tikalsky, Member \_\_\_\_\_  
Date Approved

and by Chris P. Pantelides, Chair of  
the Department of Civil and Environmental Engineering

and by Donna M. White, Interim Dean of The Graduate School.

## ABSTRACT

Corrosion of reinforced concrete is a major concern in the United States infrastructure. It is possible to create corrosion resistant concrete structures through careful evaluation of the environmental and mechanical demands on the structure and by selecting appropriate materials to meet those demands. Designers, owners, contractors, and suppliers can work together to produce a concrete capable of withstanding the harsh demands of today and the future. Specifying a ternary mixture with fly ash and slag will produce a less permeable concrete which will both extend the time to corrosion initiation and decrease the rate of propagation. Furthermore, using reinforcing less susceptible to corrosion will extend the service life of the structure. Epoxy coated rebar provides a protective coating for the steel to prevent corrosion. This research seeks to demonstrate the effectiveness of using a ternary blend in conjunction with epoxy coated rebar in helping to decrease the odds of corrosion by reducing permeability and providing a protective coating for the reinforcing.

## TABLE OF CONTENTS

ABSTRACT.....	iii
LIST OF FIGURES.....	vi
LIST OF TABLES.....	ix
ACKNOWLEDGEMENTS.....	x
<b>1 INTRODUCTION.....</b>	<b>1</b>
1.1 Corrosion Mechanism.....	1
1.2 Life Cycle.....	4
1.3 Research Significance.....	8
<b>2 MATERIALS.....</b>	<b>10</b>
2.1 Silica Fume.....	12
2.2 Ground Granulated Blast Furnace Slag.....	13
2.3 Fly Ash.....	14
2.4 Black Steel.....	15
2.5 Epoxy Coated Rebar.....	15
2.6 Stainless Steel.....	18
2.7 Stainless Steel Clad.....	20
2.8 Galvanized Steel.....	21
2.9 Fiber Reinforced Polymer Bars.....	22
2.10 MMFX Steel.....	24
<b>3 PROCEDURES.....</b>	<b>30</b>
3.1 Mixture Design.....	30
3.2 Rebar Preparation.....	31
3.3 MIxing.....	31
3.4 Impressed Current Test.....	32
3.5 Half Cell Potential.....	33
3.6 Resistivity.....	34
<b>4 RESULTS.....</b>	<b>44</b>
4.1 Impressed Current.....	44
4.2 Half Cell Potential.....	47

4.3 Resistivity .....	48
5 CONCLUSIONS.....	67
REFERENCES .....	70

## LIST OF FIGURES

Figure	Page
1 Corrosion of steel in concrete (FHWA) .....	9
2 Corrosion stages (Tuutti, 1982).....	9
3 Stainless steel reinforcing.....	29
4 Galvanized rebar.....	29
5 MMFX Reinforcing.....	29
6 Undamaged ECR bars .....	38
7 ECR end cut.....	39
8 ECR with pinhole damage.....	39
9 ECR bars with "mash" damage .....	39
10 Duplex bars as-received .....	39
11 Black bars as-received.....	40
12 SSC end cut .....	40
13 ECR and SSC pin-hole .....	40
14 Test schematic for impressed current test (Florida DOT, 2004).....	41
15 Test schematic for half cell potential test (Guthrie, 2008).....	42
16 Test schematic for resistivity test .....	43
17 Four probe resistivity schematic.....	43
18 Black bars in OPC current vs time .....	49
19 Black bar in OPC after impressed current test .....	49

20 Black bar in OPC after impressed current test .....	50
21 Black bars in ternary current vs time.....	50
22 Black bars in ternary after impressed current test .....	51
23 Black bars in ternary after impressed current test .....	52
24 Visual comparison of ternary vs OPC specimens containing black bars .....	52
25 Stainless bars in OPC current vs time .....	53
26 SSA in OPC after impressed current test .....	53
27 Visual comparison of SSA and black bars in OPC .....	54
28 Stainless bars in ternary current vs time.....	54
29 Visual comparison of OPC and ternary SSA bars.....	55
30 Clad bars in OPC as-received current vs time.....	55
31 OPC SSC bars (as recieved) after impressed current test .....	56
32 Clad bars in OPC pinhole current vs time.....	56
33 SSC bar in OPC after impressed current test .....	57
34 Clad bars in ternary endcut current vs time.....	57
35 Ternary SSC (end cut) after impressed current test .....	58
36 SSC bar in ternary (end cut) after impressed current test.....	58
37 Comparison of OPC and ternary SSC bars .....	59
38 Epoxy bars in OPC mash current vs time.....	59
39 ECR (mashed) in OPC after impressed current test .....	60
40 Epoxy bars in OPC pinhole current vs time .....	60
41 ECR (pinhole) in OPC after impressed current test .....	61
42 Epoxy bars in OPC endcut current vs time .....	61



43 ECR (endcut) in OPC after impressed current test.....	61
44 Epoxy bars in ternary endcut current vs time.....	62
45 ECR (endcut) in ternary after impressed current test.....	63
46 Half Cell Potential vs time for all the specimens studied .....	63
47 Comparison of half cell potential of different bars (as-received) in OPC.....	63
48 Comparison of half cell potential of different bars (as-received) in ternary .....	64
49 OPC and Ternary comparison of half cell potential of black bars .....	64
50 OPC and Ternary comparison of half cell potential of SSA bars .....	65
51 OPC and Ternary comparison of half cell potential of SSC bars (endcut) .....	65
52 Resistance vs time comparison of OPC and ternary .....	66

## LIST OF TABLES

Table	Page
1 Example chemical composition of typical silica fume (American Concrete Institute, 2007).....	26
2 Chemical Composition of Blast- Furnace Slags in North America (ACI, 2007)....	27
3 Example bulk composition of fly ash with coal sources (ACI, 2007) .....	27
4 Cost of Reinforcing (2008 FOB).....	28
5 Chemical Composition of Type I/II Cement and SCM.....	37
6 Mixture Proportions .....	38
7 Chemical Composition of Steel.....	38
8 Probability of Corrosion According to a Copper Copper-Sulfate Half Cell (ASTM C-876).....	42

## ACKNOWLEDGEMENTS

This educational experience and achievement would not have been possible were it not for the patience and gracious help of the faculty, staff and students at the Civil Engineering Department at the University of Utah. In particular, I would like to thank Dr. Tikalsky and Dr. Pantelides for their unwavering support in helping me get to this point. Thank you to Dr. Romero for your helpful review and suggestions and flexibility during the last few months.

I would like to thank the individual members of the concrete lab for help in preparation and testing of the specimens, Shannon Hanson, Rachel Smith, Brett Raddon and Dr. Clayton Burningham; though he did not work in the lab, he was still willing to lend a hand.

Thank you to Holcim Cement, Western Coatings, Nouvinox, & Arminox for supplying the materials for testing. Thank you to Cagley & Associates for their generous and patient support.

And, finally, thank you to my wife Melissa for all the help, understanding, and motivation.

## CHAPTER 1

### INTRODUCTION

There was a significant increase of the corrosion of reinforcing steel in the late 1960s and early 1970s that was attributed to clear roads policies of the 1960s which required the broad use of deicing salts. Salt application to cracked or porous reinforced concrete results in accelerated corrosion of the steel. These policies allowed improved safety during poor weather conditions, but changed the environmental exposure conditions of concrete highways. The application of deicing materials to most roads and bridge decks in the United States is necessary for traffic safety, but can cause corrosion and premature deterioration of the structure. Failure of some bridges and bridge decks has led to public concern for the integrity of the nation's highway system and there is an ever-increasing demand for engineers to build long life structures while using fewer natural resources. Owners and engineers alike are focusing more on life cycle costs and using materials that have greater durability and similar or slightly higher initial costs in order to achieve a long life structure.

#### 1.1 Corrosion Mechanism

Corrosion in transportation structures is an electrochemical process that provides for the oxidation and eventual reduction of structural reinforcing and prestressing steel. There are two conventional methods for mitigating corrosion in reinforced concrete: 1)

increase the time period in which the steel is protected from a corrosive environment and, 2) increase the time associated with the propagation of corrosion. Concrete is a highly alkaline environment that passively protects steel from the oxidation/reduction reactions of corrosion. Undisturbed in a moderate environment, reinforcing steel in a concrete structure may last for one hundred years or more. However, highway structures are subject to cracking from loading, freeze-thaw cycles, early age construction conditions, as well as, deicing chemicals, and a variety of other physical and environmental conditions. Deicing chemicals, particularly chloride salts, create chloride concentrations that diffuse into concrete and reach the reinforcing steel, destroying the passive protection of the alkaline concrete. Increasing the time to exposure of detrimental chloride concentrations can be achieved by reducing the permeability and diffusion properties of the concrete, controlling the size and distribution of cracks, and by the use of certain chemical admixtures in concrete. The other half of the equation is corrosion propagation. Once conditions exist to corrode steel, the speed at which the reaction occurs depends on the amount of steel surface exposed to the reactive environment and the resistance of the materials in the reactive circuit. The propagation of corrosion can be severely slowed by protective coatings over the steel, corrosion resistant alloy steel (stainless or dual phase steel), and by increasing the electrical resistance of the corrosion cell.

The steel in reinforced concrete structures is passivated by the alkaline environment in concrete. A thin oxide film forms on the steel in the highly alkaline concrete pore water and prevents the steel from further oxidizing. The alkaline environment is primarily maintained by the sodium and potassium in the pore water;

within concrete. The penetration of chloride ions or the carbonation of calcium hydroxide within concrete decreases the alkalinity over time and subsequently destroys the passivation film. Figure 1 shows that once this film is broken, oxygen and moisture reach the steel and the corrosion reaction begins, using the remaining passivated areas as cathodes and the broken film area as the anode.

Corrosion is an active chemical process that does not progress at a uniform rate. Changes in environmental conditions such as, moisture, salt concentration, temperature, and electrical current may accelerate or decelerate the rate of corrosion. In plain carbon reinforcing steel, this type of corrosion is called macrocell corrosion. This is a condition where both the anode and cathode of the cell are part of the same alloyed material. The layered pearlite structure in plain carbon steel has carbide as the cathode and ferrite as the anode. The resulting reactive cell results in iron releasing 2 electrons,  $\text{Fe} \rightarrow \text{Fe}_2^+ + 2\text{e}^-$ . The two electrons created in the anodic reaction are consumed in a cathodic reaction with water and oxygen,  $2\text{e}^- + \text{H}_2\text{O} + \frac{1}{2} \text{O}_2 \rightarrow 2\text{OH}^-$ . The flow of electrons between the anodic and cathodic areas through the steel and its counter-current flow through the concrete pore solution completes the corrosion circuit. The counter flow consists of negatively-charged hydroxide ions and positively-charged ferrous ions. Using Ohm's Law, if the concrete's electrical resistance to these ions is high, the rate of current flow carried by the ions will be low. Subsequently, the anodic and cathodic reactions will proceed slowly and the rate of corrosion will be low. The addition of pozzolans was an example of a means of increasing the electrical resistance.

The passive layer provides protection, but can be destroyed. Depassivation may occur under two specific main sets of conditions: (1) reduction of the pH below 10 due

to reaction with atmospheric CO<sub>2</sub> or CO (carbonation); or (2) penetration of chloride ions into the concrete pore solution at the level of the steel. Once depassivation occurs, the steel is no longer protected and corrosion may be initiated. CO<sub>2</sub> and CO from the environment or chlorides from deicing salts or seawater diffuse into the concrete over time and react with the hydroxide and calcium ions in the pore solution. Even when the concrete pore water solution pH level remains high, chloride ions in high concentrations can still effectively depassivate the steel. Chloride ions may diffuse into the concrete or be introduced in the concrete mixture from an admixture, such as the accelerator CaCl<sub>2</sub> or in chloride-contaminated aggregates or mixing water. When carbon dioxide molecules penetrate into reinforced concrete, it reacts with calcium hydroxide in the pore solution and decrease the alkalinity of the pore solution. This reaction creates carbonates and water which evaporates, causing carbonation shrinkage and may create microcracks that permit further carbon dioxide and chloride ingress. Carbonation usually penetrates slowly into the concrete member to the level of the reinforcing steel. The time it takes this front to reach the steel is a function of the depth of the cover and of the rate of diffusion of the atmospheric CO<sub>2</sub> and CO into the concrete.

### 1.2 Life Cycle

Service life of a structure or the reinforcing steel in a structure can be illustrated by the model shown in Figure 2. It is comprised of an initiation stage (time of completion to time chloride threshold is reached and initial oxidation takes place) and the propagation stage (after initial oxidation to the end of service life). The initiation stage is dependent on many variables, including environment, chloride exposure, cover, and concrete type. In poor or cracked concrete, the initiation stage may be a matter of years,

however, in properly designed and constructed concrete it may be decades and in HPC it can be a century or more. The length of the propagation phase depends on the corrosion rate after the chloride threshold is reached. Corrosion rate may vary considerably depending on the resistivity of the concrete, the oxygen and moisture availability, alloy of the steel, and the environmental conditions. The end of service life is defined by the user.

Though models for chloride ingress, carbonation, and corrosion development have been studied (e.g. COLLEPARDI et al., 1972, BODDY et al., 1999, BENTZ et al., 2001, ALISA et al., 1999, PAPADAKIS et al., 1992, 2000, ŠMERDA et al., 1992) including those from the probabilistic standpoint (KERŠNER et al., 1996, TEPLÝ et al., 1999, DAIGLE et al., 2004, THOFT-CHRISTENSEN, 2005), there are still many issues that must be addressed for them to become useful engineering tools, especially with regard to reliability models that can be readily used by agencies and professionals.

Diffusion is the primary means by which chlorides penetrate to the level of reinforcing steel to initiate corrosion. The effects of hydraulic pressure and capillary absorption are minor in comparison in most cases and rarely driving factors in highway structures. It is widely accepted that Fick's 2<sup>nd</sup> law of diffusion can represent the rate of chloride penetration into concrete as a function of depth and time (Konecny et al., 2006). The solution (referred to as the Crank Solution) of the governing differential equation is given as Equation (1) (Collepari et al., 1972)

$$C_{x,t} = C_0 \left[ 1 - \operatorname{erf} \left( \frac{x}{\sqrt{4D_c t}} \right) \right] \quad (1)$$

where  $C_{x,t}$  is the concentration of chlorides (percent by mass of total cementitious materials) at time  $t$  (years) and depth  $x$  (meters),  $C_0$  is the concentration of chlorides (% by mass of total cementitious materials) at the surface directly inside the concrete, and  $D_c$



is the apparent diffusion coefficient ( $\text{m}^2/\text{year}$ ). Equation (1) is widely used for chloride ingress models but does not account for cracks and must be modified to account for time-dependent changes in material property or boundary conditions.

Severity of the chloride ingress can be assessed by comparing the chloride threshold value at which corrosion initiates,  $C_{th}$ , with the chloride concentration at the exposed areas of reinforcing steel. This value will depend on the type and preparation of the reinforcing steel and the constituents of the concrete as well as other factors. Typical values are 0.2 percent chlorides by mass of total cementitious materials according to ACI 207R-01 and 0.4 percent in the Eurocode 3 on Concrete Structures. The reliability,  $RF_t$ , of a bridge deck is expressed as the time-dependent exceedance of the corrosion threshold by the location-dependent chloride concentration,  $C_{xy,t}$ . The reliability function characterizing the above-described limit state is expressed as:

$$RF_t = C_{th} - C_{xy,t} \quad (2)$$

Probabilistic time-dependent analysis can be thought of as a comparison of the joining extrema of the chloride concentration  $C_t$  and threshold  $C_{th}$  random realizations. Once the probability that the chloride concentration at the reinforcing steel level exceeds the threshold by a user-defined amount (dependent on structure importance), corrosion is assumed to begin and the structure is designated as unreliable in terms of further delaying the onset of corrosion.

Konecny et al. (2006) provide the most advanced model for understanding the ingress of chlorides and the related factors. Using simulation-based reliability assessment (SBRA) with finite elements, Konecny et al. were able to show that concrete with large

cracks and poor quality ECR coating have marginal service lives, but concrete with thin cracks and ECR that meets minimum quality control standards have long service lives.

Life 365 is an easy-to-use computer program that can help compare alternatives for new construction and estimate remaining service life of existing structures. Engineers can use the data obtained from nondestructive test methods such as, resistivity and half cell potential, as input to predict accurately service life for concrete structures. Life 365 is not without limitations. For example, Life 365 does not account for initial cracking which can allow a direct pathway for chlorides, air, and moisture at the reinforcing level. This can greatly reduce the time to corrosion initiation.

The Life-365 service-life model computer program estimates life cycle costs (LCC) of reinforced concrete as affected by chloride corrosion of reinforcement. The development of the program was initiated by the Strategic Development Committee of ACI for the purpose of developing a “standard model” for LCC (Clausen 2004). The program is available at no cost and can be a great resource for designers and owners.

There are many variables in service life prediction of bridge decks and other reinforced concrete structures. Construction practices, materials, and exposure conditions all affect the service life of the structure and need to be included in the model. Current life cycle predictions are based on the limited available data. Several assumptions and approximations are necessary in order to compare alternatives and analyze existing bridges. These assumptions and approximations affect the accuracy of the prediction and analysis and need to be accounted for in the model. Identifying the significant variables and the insignificant variables poses a challenge to researchers.

### 1.3 Research Significance

The purpose of this research is to compare the available reinforcing materials and to show the effect of supplementary cementitious materials on the resistivity of the concrete, which will increase the time to corrosion initiation and extend the propagation period. This has useful life implications for reinforced concrete structures exposed to chlorides and moisture. This study uses different corrosion resistant alternative reinforcing and compares their half cell potential and the time to failure of the impressed current test specimens made from concrete with different technical properties. Resistivity results and comparisons will show the difference between mixtures with supplementary cementitious materials and those without.

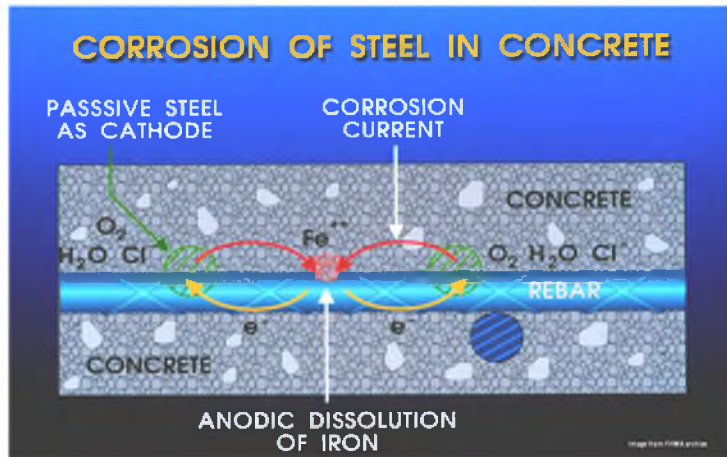


Figure 1 Corrosion of steel in concrete (FHWA)

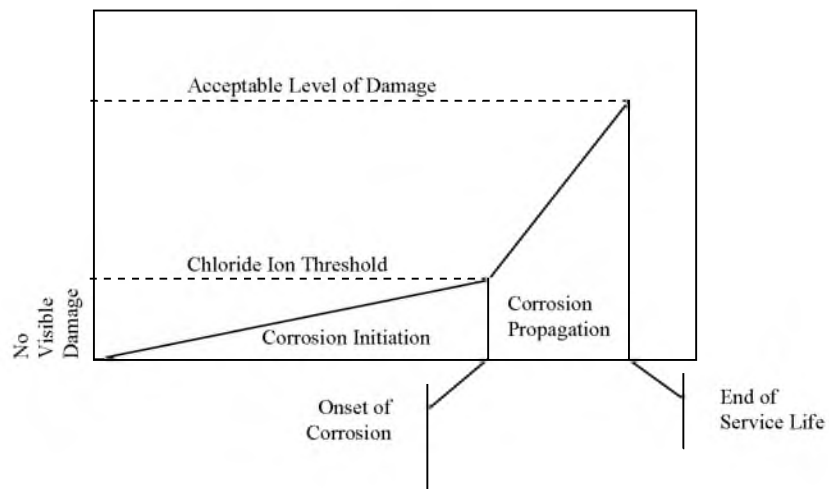


Figure 2 Corrosion stages (Adapted from Tuutti, 1982)

## CHAPTER 2

### MATERIALS

The concrete mixture design and material selection is important in protecting reinforced concrete from corrosion. Proper selection of materials will increase the time to corrosion and decrease the rate of corrosion propagation, thereby effectively increasing service life of the structure. There are few factors that should be considered when choosing the appropriate materials for any specific project; the most important of which being anticipated service life. The designers, contractors, and owners can work together to produce a concrete structure that will meet the anticipated demands by specifying proper materials and construction methods. The use of trial batches and preconstruction testing data can help ensure that the anticipated service life will be achieved.

Protecting the steel in reinforced concrete can be achieved by using a corrosion resistant steel, increasing concrete cover, providing a corrosion inhibiting admixture, sealing the concrete, and/or by creating a less porous concrete. Two methods of protecting the steel using materials will be discussed and evaluated; first, creating a dense concrete matrix by using supplementary cementitious materials and then using corrosion resistant steel.

Mixtures with supplementary cementitious material replacement will increase the time required for the chlorides to diffuse to the level of the reinforcing in a sufficiently high concentration to initiate corrosion by creating a less porous concrete matrix.

The primary cementitious material in most structural concrete applications is portland cement. Portland cement is an inexpensive hydraulic cement manufactured at high temperatures from limestone, clay, and gypsum. Pozzolans and slag cement can be added to concrete mixtures with portland cement as “supplementary cementitious materials (SCM).” While some SCMs are hydraulic cements by themselves, they typically provide a better product when blended with portland cement. The use of SCMs can provide a potential economic advantage. Fly ash and natural pozzolans typically cost less than portland cement. When optimized, the total cost of portland cement with supplementary cementitious materials is likely less than a mixture with portland cement alone.

Pozzolans are a special class of cementitious materials that use the excess calcium hydroxide from the reaction of portland cement to generate more cementing compounds. The result of such reactions is a tighter matrix of cementing compounds that has a lower permeability. There are several advantages to using pozzolans with portland cement in concrete:

- Reduced permeability
- Reduced cost
- Lower heats of hydration
- Increased resistance to alkali silica reaction (ASR)
- Increased resistance to sulfate attack
- Lower carbon footprint
- Higher long-term compressive strengths
- Increase workability during construction

There are several types of pozzolans, including high calcium fly ash, low calcium fly ash, silica fume, and blast furnace slag. All these pozzolans affect the properties of the fresh and hydrated concrete.

The use of these supplementary cementitious materials can affect the cementitious materials ratio (w/cm) which is an important factor in producing concrete that is resistant to corrosion. Lower w/cm will result in fewer internal voids in the concrete and a more dense microstructure in the concrete paste. This refined microstructure has a lower diffusion constant and a higher resistance to electrical current. Both of these properties are advantageous to protecting steel from the effects of corrosion.

In addition to reducing cost and providing corrosion resistance, the use of some pozzolans or SCMs may add workability to the concrete and require less total water or water reducing admixtures. This is especially true for fly ash due to spherical shape of the particles. Using fly ash as a partial cement replacement will also provide greater finishability due to a tighter pore structure, less bleeding, and increased constituent cohesion. To determine the proper dosages and the interaction of fly ash with portland cement, the designer and ready-mix supplier should prepare trial batches to ensure material compatibility in both the fresh and cured concrete state.

### 2.1 Silica Fume

Silica fume, or microsilica, is a byproduct of ferro-silicon-metal production. Silica fume is much finer grained than portland cement with an average diameter of 0.1  $\mu\text{m}$ . Silica fume generally contains over 90% silicon dioxide and has a specific gravity in the range of 2.10 to 2.55 (American Concrete Institute, 2007). Silica fume concrete was first used in highway applications in the United States in the mid-1980s. Since that time, the

use of silica fume concrete has grown considerably. Silica fume is typically used as a small percentage of total cementitious materials, e.g., 3-8% of total cementitious material. It costs 6 to 10 times the cost of portland cement and therefore must be used judiciously to be economical. The fine particle size often increases water demand, but also allows it to enter into the cementitious reactions sooner than other materials. It is recommended that silica fume concrete be made with a high-range water-reducing (HRWR) admixture. Concrete containing silica fume rarely bleeds and therefore it must be wet cured from the time of placement to prohibit early age cracking.

Silica fume affects concrete by lowering the permeability and diffusion constants, increasing early age strength, delaying the onset of ASR, and providing a sticky adhesive characteristic to fresh concrete. These characteristics are ideal for protecting steel from a corrosive environment. However, the sensitivity of concrete containing silica fume to curing conditions and early age cracking is a detriment to creating a corrosion resistant structure. Although these can be controlled through good concrete practices, the potential exists for early age cracking which is a direct pathway for chlorides and moisture. The typical chemical composition of silica fume is shown in Table 1.

## 2.2 Ground Granulated Blast Furnace Slag

Blast furnace slag is a byproduct of iron production. When the slag is ground and granulated shortly after being produced, it is both a hydraulic cement and a pozzolan. It requires only about 3% of the CO<sub>2</sub> to manufacture a slag cement as it does to manufacture a portland cement. Slag is typically 95% silicates, aluminates, and calcium. It can be used as a portion of the cementitious material in concretes with proportions ranging from 35 ~ 70 percent by mass of total cementitious material. Slag cement



inclusion reduces heat evolution, environmental impacts, and susceptibility to ASR and sulfate attack. The addition of ground granulated blast furnace slag (GGBFS) may also reduce the amount of HRWR required to attain the same flowability as a mixture containing only portland cement. Creep and shrinkage of concretes containing slag cement are not significantly different from concretes not containing slag cements. The typical chemical composition of GGBFS is shown in Table 2.

### 2.3 Fly Ash

Fly ash is a by-product of coal combustion and has been used as a partial replacement of cement since the 1930s. Fly ash can improve the chemical resistance of the concrete, lower the heat of hydration, increase long-term strength, increase workability, reduce permeability, provide sulfate resistance, and mitigate alkali silica reaction. The typical chemical composition of both class F and class C fly ash is shown in Table 3. The primary difference of class F and class C fly ash is the amount of CaO. Class F fly ash typically has less than 10% CaO and is derived from bituminous or anthracitic coal. Class C typically has more than 20% CaO and is derived from a sub bituminous coal. Typical dosages of fly ash are 20 ~35%.

There are many different types of reinforcement available for reinforced concrete. The cost and value of different materials is largely dependent on the design and in-service exposure conditions. The most common is “black” steel rebar. This is steel meeting ASTM 615. Galvanized and epoxy coated rebar are often used in concrete exposed to corrosive environments. There are experimental bars and bars that have not been widely available until recently, including glass and carbon fiber reinforcing bars, stainless steel rebar, and stainless clad rebar. The costs of these materials vary with market conditions.

The April 2008 FOB costs in Salt Lake City, UT are listed in Table 4.

#### 2.4 Black Steel

Black steel meeting a minimum ASTM A615 has the lowest initial cost of all the reinforcement considered. Black steel has tensile strengths usually 60 and 75 ksi and is suitable in applications where the structure will not be exposed to corrosive environments. Corrosion resistance for black steel is gained by the passivating high alkaline environment that limits the oxidation of the steel. The passivation will be compromised and corrosion begins when a chloride ion concentration of greater than 0.4% occurs at the level of reinforcement. For mixtures that resist chloride ion penetration for the projected life of the structure, black steel may be an acceptable design choice. Many southern state DOTs specify black steel for certain projects due to the mild exposure conditions. The black steel can last between 20~100 years before replacement, depending on the environment, cover, salt application, etc. With the proper cover and HPC with little cracking, black steel could potentially serve an average 75-year life for a structure in applications with low to moderate exposure to deicing salts.

#### 2.5 Epoxy Coated Rebar

Epoxy coated rebar (ECR), ASTM A775, is currently the most commonly specified reinforcement by state DOTs for structures exposed to chloride salts. The Federal Highway Administration (FHWA) and the NBS National Bureau of Standards (NBS), now National Institute of Standards and Technology (NIST), began testing organic coatings to protect the steel reinforcement from the corrosive effects of deicing salts in the 1970s. In 1973, the Pennsylvania Department of Transportation started experimenting with ECR and in 1976 implemented it into all of their bridge work. Since

then, nearly every northern tier state DOT has adopted ECR in applications with exposure to chloride salts. The Pennsylvania and the New York DOT have not yet replaced a single bridge because of corrosion of ECR. ECR has some advantages and disadvantages in its material characteristics when used in concrete structures:

- Advantages
  - Relatively inexpensive.
  - Coating that protects the steel from the corrosive environment.
  - Readily available in most areas.
  - Quality control appears to be improving.
- Disadvantages
  - Holidays can cause concentrated areas of corrosion.
  - Special handling precautions are required to avoid damaging coating.
  - Adhesion between the coating and the steel decreases over time.

While the ECR has certainly shown isolated areas of distress, it largely has served much longer than black bar. Premature corrosion of ECR in Sunshine Skyway Bridge in Florida has created questions about the long-term performance of ECR in marine environments (Hartt, Lysogorski, & Leroux, 2004); however, other states have not experienced the same magnitude of distress. Flexible epoxy coatings are typically colored green and can be bent or shaped after the coating has been applied. Grey, red, or purple colored coatings are typically non-flexible coatings that are to be applied after the bars have been bent or cages assembled.

Epoxy-coated reinforcement has gained mainstream acceptance since the early 1980s as a means to extend the useful life of highway structures. The epoxy coating

prevents moisture and chlorides from reaching the surface of the reinforcing steel by acting as a barrier. Research to date estimates additional service life between 40 to 50 years with plain portland cement concrete and ECR. When ECR is used in conjunction with high-performance concrete (HPC) service lives may be expected to be 85 to 100 years. Generally, the performance of ECR has been good. However, no ECR structures have been in service long enough to evaluate the actual service life, only estimates can be made. Bridges in Pennsylvania and New York have been in service for more than 30 years with no signs of corrosion of the reinforcing steel (Camisa and Tikalsky, 2005) and bridge decks in Iowa have been reported to have lasted 20 years and counting (Jolley, Fanous, Phares, & Wipf, 2005).

The corrosion protection for ECR, compared to that of black steel, is only as good as the coating. Bars need to be handled with care in order to prevent damaging the coating which would reduce the corrosion resistance of the bars greatly. Nearly all research (e.g. Humphreys, 2004; Konecny, Tikalsky and Tepke, 2007; Jolley, Fanous, Phares, & Wipf, 2005; Lee, and Krauss, 2004; Camisa and Tikalsky, 2005; Cui and Krauss, 2006) with the exception of that conducted by Brown et al. (2003) have found the ECR substantially increases the life of bridges and structures. While the research indicates a gradual loss of adhesion between the bars and the coating over time, the steel does not disintegrate in the same manner as black steel. Even Brown et al. report a 12% increase in life with an increase to the overall cost of the bridge of less than 1%.

## 2.6 Stainless Steel

Stainless steel has long been considered cost prohibitive based on an initial cost. With more agencies considering life cycle costs, stainless steel can be a competitive

alternative to traditional cost, despite the higher initial cost. Stainless steels not meeting ASTM C 955 should not be considered.

Stainless steel, as shown in Figure 5, typically contains between 15-30% chromium and has very high resistance to corrosion. Rapid corrosion tests, performed by many different researchers, consistently rank stainless steels to have the highest resistance to corrosion (Yunovich, 2004, Hartt, 2006). Due to the high cost, this alternative has not been widely used. There are several different types of stainless steel. ASTM C 955 allows for 6 types for use in reinforced concrete. Each has different corrosion properties, as shown in Figure 6.

- 1) 2201
- 2) 205 typically \$3.50 per pound
- 3) 304
- 4) 316
- 5) 316LN typically \$4.50 per pound
- 6) 3Cr12

The stainless steel reinforcement has some advantages and disadvantages in its material characteristics when used in concrete structures:

- Advantages
  - High corrosion resistance
- Disadvantages
  - Highest cost
  - Some concerns about ductility

A recent study concluded that the use of stainless steel (316LN) reinforcing bar is

the preferred recommendation as the bridge deck corrosion protection system under the most severe exposure conditions (Hartt, 2006). The use of stainless steel (316LN) reinforcing steel is also recommended for coastal substructures. That same report demonstrated that the additional cost of stainless steel reinforcement is less than the cost of a single rehabilitative overlay for a bridge deck that does not reach 75-year design life and that stainless steel reinforcement may be implemented selectively for decks subject to the most severe exposures (Brown, Weyers, & Via, 2003). Stainless 2201 and 2205 steel alloys were used in Florida (Hartt, Powers, Lysogorski, Liroux, & Virmani, 2007) with excellent corrosion resistance as measured by accelerated corrosion tests.

There are several steel mills that are producing limited runs of low-cost, corrosion resistant grades of chromium alloy steel. These steels are usually a dual phase, mid-chromium alloy designed to have similar corrosion resistant properties as high chromium alloys. Several new steels are available at reasonable costs which could potentially reach 100 year service life. These new steels should be investigated to ensure that the properties are appropriate for use as reinforcement in concrete structures. Enduramet32™ and MMFX are new grades of duplex steel that claim good corrosion resistance and performed well in certain types of preliminary tests. Enduramet32™ will sell for around \$2.90/ lb. Arminox™ steel also has a new grade of duplex steel for around the same price. Further investigation into the properties of the new steel is recommended before specifying the material.

## 2.7 Stainless Steel Clad

Stainless steel clad (SSC) rebar is currently produced by two known processes. In one of the processes, stainless steel strip is formed and welded into a tube shape. Carbon

steel granulate is then packed under pressure into the tube to form the core. The ends are crimped to complete the “manufactured” round billet. The billet is then heated and rolled into reinforcing bars. In the other existing process, a carbon steel continuous cast billet is spray metallized with a stainless alloy cladding. Then the billet is heated and rolled into reinforcing bars.

Several DOTs have used stainless steel clad experimentally, e.g., Kentucky, South Carolina, Virginia, West Virginia, Wisconsin, Oregon, Florida, and South Dakota. The SSC rebar estimated to give 50-60 years of life before damaging the concrete. Abrading the cladding reduced the life estimate by a few years, usually 1-5 years. Drilling a hole in the cladding, to simulate a break, significantly reduced the estimated life of the end coated SSC rebar by 15-40 years (Cross, Duke, Kellar, Han, & Johnston, 2001; Clementa, 2004).

The SSC reinforcement has some advantages and disadvantages in its material characteristics when used in concrete structures:

- Advantages
  - Corrosion resistant layer
  - Less expensive than solid stainless steel but similar corrosion resistant properties
  - High life expectancy under ideal material properties
- Disadvantages
  - High cost
  - Nonuniform thickness of cladding
  - Defects can cause concentrated areas of corrosion. Carbon steel is less noble than stainless and therefore will corrode in preference to the

stainless steel.

- Different metals with slightly different coefficients of expansion.
- Dissimilar metals in direct contact.
- Gaps between the cladding and the core.
- Supply may not meet demand.
- Requires special treatment of the exposed ends.

There have been reports of potential problems with the uniformity of the thickness of the cladding. Studies conducted by South Dakota DOT, Florida DOT, and Oregon DOT found that the yield strength may actually be less than required by specs for ¾” bars. There are also production limitations restricting smaller diameter bars. Separation of the cladding from the core is also a concern. There have also been reports of significant delays in delivery schedules.

## 2.8 Galvanized

Hot dip galvanizing is a process that applies a zinc coating to the steel rebar by immersing the bars in molten zinc (about 450° C). This creates a coating consisting of an inner core of the base steel, a steel zinc alloy layer, and an outer layer of pure zinc.

- Advantages
  - Relatively inexpensive (\$0.50~\$0.60 /lb)
  - Higher threshold for initiation of corrosion
  - No special handling requirements
  - Much greater adhesion than ECR
- Disadvantages
  - Possibility of reaction of the metal with concrete to produce hydrogen gas



- Only provides corrosion resistance until zinc is consumed

Galvanized steel is being used by several transportation agencies. Galvanized steel has a sacrificial zinc coating that will corrode without expanding. However, after the sacrificial layer is gone, corrosion of the black steel core begins (Yeomans & Novak, Further Studies of the Comparative Properties and Behaviour of Galvanized and Epoxy Coated Steel Reinforcement, 1990). The corrosion products of the zinc are not expansive, therefore they do not create the same internal stresses as the corrosion products of iron. Galvanized steel delays the onset of corrosion (Yeomans S. R., 1991).

### 2.9 Fiber Reinforced Polymers

In recent efforts to solve the corrosion problems in concrete, nonmetallic materials such as fiber reinforced polymer (FRP) composites have become an alternative to reinforcing steel in various concrete structures. FRP reinforcement is primarily made of fibers embedded in a thermosetting polymer or thermoplastic resin. The small diameter inorganic and organic fibers (e.g., glass, carbon, aramid, and polyvinyl alcohol) provide FRP reinforcement with strength and stiffness, whereas the polymer resins (e.g., polyester, vinyl ester, and epoxy) bind the fibers together. In addition, inorganic fillers (e.g., calcium carbonate, clay, and alumina trihydrate) can be mixed with the resins for cost reduction, property modification, and processing property control of FRP reinforcement.

The FRP reinforcement has some advantages and disadvantages in its material characteristics when used in concrete structures:

- Advantages
  - High longitudinal strength

- Nonmagnetic
- Corrosion resistance
- High fatigue endurance
- Light weight
- Reduced lap splices because of the availability of 40' length bars
- Low thermal and electric conductivity
- Disadvantages
  - No yielding before brittle rupture
  - Low transverse strength
  - Low modulus of elasticity
  - Susceptibility to damage due to ultra-violet radiation
  - Low durability of some glass fibers in a moist environment
  - Low durability of some glass and aramid fibers in an alkaline environment

The material characteristics of FRP need to be carefully considered when determining whether FRP reinforcement is suitable or necessary for a particular concrete structure. There are several commercially available FRP reinforcements made of continuous aramid (AFRP), carbon (CFRP), or glass (GFRP) fibers embedded in various resin materials. Also, FRP reinforcements can be sorted by the type of surface deformation system, such as exterior wound fibers, sand coating, or separately formed deformation (Nanni & Faza, 2002). The price of FRP bars has decreased and now can be competitive with ECR. The construction of an FRP reinforced bridge deck may actually cost less than the same deck reinforced with ECR. Wisconsin DOT reported a 57% savings in man hours required to place the bars because of the low weight of the material

(Berg, Bank, Oliva, & Russell, 2006). There is also less of a demand for impervious concrete and strict curing procedures so there could be a reduction in cost associated with that. Also, many manufacturers can supply the bars in 40' lengths, thereby reducing the number of lap splices and saving additional materials. However, longer lap splices are required for the same diameter FRP bar than a steel bar.

### 2.10 MMFX

MMFX steel is a low carbon steel containing about 9% chromium (ASTM 1065). The technology was developed roughly 10 years ago (Darwin, Browning, Nguyen, & Locke, 2002), and has received considerable attention from the transportation industry. Reports from the MMFX technologies and various DOTs and Universities rate the corrosion resistance from moderate to excellent. MMFX did not perform well in a salt fog study (Darwin, Browning, Nguyen, & Locke, 2002) and the Florida DOT has not completed its evaluation. Because MMFX is a relatively new technology, no long-term performance data exist. MMFX has a tensile strength of 100 ksi and an ultimate strength of 120 ksi.

The MMFX reinforcement has some advantages and disadvantages in its material characteristics when used in concrete structures:

- Advantages
  - Relatively low cost.
  - High strength.
  - Corrosion resistance.
- Disadvantages
  - Only one supplier.

- No specifications exist.
- No long-term data exist.
- Corrosion resistance may not be sufficient.

Predicted useful life of RC structures using MMFX steel varies from 55- 100 years. These predictions are based on accelerated corrosion tests. A study conducted by the Kansas DOT in conjunction with South Dakota DOT reported that ECR actually performed better in Accelerated Corrosion Tests (ACT) than MMFX. Figure 5 displays some of the results of the study. Most other studies conclude that the corrosion resistance of MMFX is equivalent or better than ECR.

There is only one supplier for the product and supply and cost have been concerns. The research to date indicates a corrosion resistance typically four to eight times that of uncoated reinforcement, and a one-third to two-thirds lower corrosion rate. That translates to an initial bridge deck service life estimate of 52 years before repairs are needed. Life cycle cost analysis over a 90-year analysis period indicated a \$31/yd<sup>2</sup> lower cost of MMFX compared to ECR.

When specifying a material to use for reinforcement, knowledge of the use of the structure, the environment, and the design service life is critical. During accelerated corrosion tests, most rebar show signs of some corrosion. Corrosion resistant reinforcement along with less permeable concrete and other measures can produce durable structures with a 100 year service life or better (Yeomans S. R., 2002). Life cycle cost analysis is the preferred method for choosing appropriate alternatives and indirect costs should also be considered. As use for some of these corrosion resistant reinforcement increases, the cost is expected to decrease and the availability to increase.

Table 1 Example chemical composition of typical silica fume (American Concrete Institute, 2007)

Chemical (%)	Silica Fume
CaO	0.42
SiO <sub>2</sub>	97.90
Al <sub>2</sub> O <sub>3</sub>	0.18
Fe <sub>2</sub> O <sub>3</sub>	0.07
MgO	0.21
K <sub>2</sub> O	0.59
Na <sub>2</sub> O	0.12
SO <sub>3</sub>	0.17
P <sub>2</sub> O <sub>5</sub>	0.12
TiO <sub>2</sub>	----
SrO	0.01
Mn <sub>2</sub> O <sub>3</sub>	0.03
LOI	----
BaO	0.02
S	----
ZnO	0.08
Cl	0.09

Table 2 Chemical composition of blast-furnace slags in North America (ACI, 2007)

Chemical Constituents (as oxides) <sup>C</sup>	Range of Composition, % by mass
SiO <sub>2</sub>	32 ~ 42
Al <sub>2</sub> O <sub>3</sub>	7 ~ 16
CaO	32 ~ 45
MgO	5 ~ 15
S	0.7 ~ 2.2
Fe <sub>2</sub> O <sub>3</sub>	0.1 ~ 1.5
MnO	0.2 ~ 1.0

Table 3 Example bulk composition of fly ash with coal sources (ACI, 2007)

	Bituminous (F)	Sub-bituminous (C)	Northern lignite (C)	Southern lignite (F)
SiO <sub>2</sub>	45.9	31.3	44.6	52.9
Al <sub>2</sub> O <sub>3</sub>	24.2	22.5	15.5	17.9
CaO	3.7	28.0	20.9	9.6
MgO	0.0	4.3	6.1	1.7
SO <sub>3</sub>	0.4	2.3	1.5	0.9
Fe <sub>2</sub> O <sub>3</sub>	4.7	5.0	7.7	9.0
Na <sub>2</sub> O	0.2	1.6	0.9	0.6
LOI	3.0	0.3	0.4	0.4

Table 4 Cost of Reinforcing (2008 FOB)

Type of Reinforcement	Price (\$/lb)
Black Mild Steel	0.45-0.55
Galvanized	0.55-0.65
Epoxy Coated	0.70-0.80
FRP*	0.70-0.75 <sup>A</sup>
Stainless	2.50-5.00
Stainless Steel Clad	2.50-3.00 <sup>B</sup>
MMFX	0.70-0.80

<sup>A</sup>Price of FRP (\$/ft) equivalent to a #5 bar in bulk      <sup>B</sup>Fabricated Price



Figure 3 Stainless steel reinforcing



Figure 4 Galvanized rebar



Figure 5 MMFX Reinforcing



## CHAPTER 3

### PROCEDURES

#### 3.1 Mixture Design

Mixture proportions for the research were consistent with those used for bridge decks. Table 6 shows the mixtures used in this study. A water cementitious ratio of 0.45 was selected with a target slump of 3” and air content of 6%. The first mixture contained only Type I/II cement as the cementitious material. The second mixture had a 20% replacement by weight of the cement by class F fly ash and 20% replacement of ground granulated blast furnace slag.

Type I/II cement, as defined by ASTM C 150, was obtained from a local cement plant and had a specific gravity of 3.15. The chemical composition is listed in Table 5.

An air entraining admixture meeting ASTM C 260 was used in the mixture in order to achieve the target 6% air. The air entrainer used was MVBR manufactured by BASF. Ground granulated blast furnace slag meeting ASTM C 989 and Class F fly ash meeting ASTM C 618 were used as a supplementary cementitious material to test the resistivity and corrosion resistant properties of a ternary mixture. The chemical composition of the fly ash and GGBFS is listed in Table 5.

A poly carboxylate high range water reducing admixture meeting ASTM C 494 was used in order to get the desired workability and slump. Aggregates meeting ASTM C 33 from local sources were used in the mixtures.

The tests and methods described are intended to give a rapid assessment as to the corrosion resistance of different readily available reinforcing steels. Different steel requires special handling or special fabrication in order to protect the corrosion resistant coatings. Improper handling in the field can damage the coating and create concentrated areas of corrosion. The following preparations are intended to simulate the most commonly encountered damage scenarios in the field.

### 3.2 Rebar Preparation

For the ECR, three conditions were tested: end cut, pin hole, and “mash.” The pinhole specimen is designed to simulate a “holiday” and the “mash” and “end cut” specimens are meant to simulate improper handling procedures. The duplex bars meeting ASTM A995 and plain black bars meeting ASTM A615 were tested as-received.

Stainless steel clad bars were tested in 3 conditions, as-received, end cut, and a pin hole. The bars were received from a manufacturing plant in England. The clad bars are fabricated and shipped to the job site. The cut end is meant to simulate a contractor making a field cut and not repairing the cut end. The clad bars had an average thickness of the cladding of 690  $\mu\text{m}$ . The cladding meets ASTM A276 and is classified as 316L

### 3.3 Mixing

Cylinders were prepared following ASTM C 192. Air content tests ASTM C 137 and slump tests ASTM C 143 were then performed to ensure that the fresh concrete met the desired requirements.

### 3.4 Impressed Current Test

As described in the introduction, corrosion is an electrochemical process that can be accelerated by impressing a current from the anode to the cathode. Florida DOT has developed test procedures to investigate different corrosion protection properties of concrete mixtures and reinforcing materials, known as “Florida Method of Test for An Accelerated Laboratory Method for Corrosion Testing of Concrete Using Impressed Current” (FDOT, 2004). This test compares various protective coatings, rebar claddings, and alloys in addition to comparing different concrete mixtures.

Metallic reinforcing bars to be tested are cast into the center 4”x8” cylinders with 1.75” of cover (see Figure 17). Specimens are cured at room temperature for approximately 24 hours before being removed from the mold and then allowed to cure in a moist room for 28 days. The bar size used is #4 or #5.

The exposed bars in the specimens were then connected to a 0.01 ohm manganin wire shunt 6A capacity Agra Engineering Holloway type RS, which was connected to the positive output of a DC power supply with a voltage of 6V (see Figure 17). The negative terminal of the power supply was connected to a number 5 bar placed at the bottom of the tank. The amperage was measured on a daily basis was measured until a visible crack formed or a large current increase was measured ( $\approx 1$  mA or greater). The large current increase would indicate significantly less resistance of the specimen. Less resistance of the system would likely be caused by degradation or cracking of the surrounding concrete caused by the formation of expansive corrosion products.

Each specimen was tested for 60 days or until failure and the results are summarized in the next section.

### 3.5 Half Cell Potential

The rate at which the half cell corrosion reaction occurs is related to the half cell potential, measured in volts. Potentials will affect the intensity of the corrosion at the anode when the external circuit is completed. The schematic for a half cell potential test is shown in Figure 18. ASTM C 876 includes a copper-copper sulfate half cell, connecting wires, and a high impedance voltmeter (usually greater than  $10M\Omega$ ) so that very little current is flowing. The copper-copper sulfate half cell consists of a copper rod immersed in a saturated copper sulfate solution. The positive terminal of the voltmeter is connected to the embedded reinforcing bar, while the negative terminal is connected to the copper-copper sulfate half cell. The copper-copper sulfate half cell is electrically connected to the concrete using a porous plug and a moistened sponge. Excess electrons at the surface of the bar have the tendency to flow from the bar to the copper-copper sulfate electrode. Excess electrons at the surface of the bar cause negative voltage readings and the more negative the reading, the more likely that corrosion is occurring.

The magnitude of the potential can be affected by different factors. Results need to be calibrated and care should be taken when evaluating concrete containing coated reinforcing, saturated specimens, and carbonated concrete (Maholtra, 2004).

The purpose of the half cell potential test is to compare the corrosion activity of different specimens. Variations in chloride concentration, moisture, and oxygen at different locations along a reinforcing bar cause voltage differentials to occur, which in turn can greatly increase the rate of corrosion. This nondestructive test method is particularly useful because it can be used to determine the probability of corrosion before damage shows at the surface of the concrete. Nondestructive test methods can help

engineers and owners make important rehabilitation decisions and estimate the service life of highway structures before damage becomes evident.

Implementing an inspection or quality control routine that includes non-destructive testing such as, half cell potential and resistivity measurements can give rapid results and help make important decisions about which materials to use and which materials to avoid. Strong electrical potential gradients will increase the current flow from the anodic site to the cathodic site and increase the rate at which the corrosion propagates. Measuring this can help quantify the corrosion activity and the corrosion resistant materials. Half cell potential measurements, according to ASTM C 876, were done every three days on specimens during the impressed current phase of the investigation.

### 3.6 Resistivity

After reinforcing steel has been depassivated, the corrosion rate is dependent on the availability of oxygen for the cathodic reaction. The rate is also largely dependent on the electrical resistance of the concrete. Less resistance will allow for the transport of ions from the anode to the cathode more easily and therefore a faster rate of corrosion. Basic electrical resistance is given by the equation:

$$R = \rho \frac{L}{A} \quad (3)$$

where R is the resistance of a conductor of area A and length L and  $\rho$  is the resistivity.

The schematic for resistivity measurements is shown in Figure 20.

$$\rho = \frac{2\pi sV}{I} \quad (4)$$

The equation above is derived based on the assumption that the material is semi-infinite and homogenous. The electrode spacing plays a significant role in the resistivity reading obtained, especially when considering the maximum size of the aggregate. Embedded rebar can also affect the resistivity. Larger aggregate will require larger spacing of the electrodes. The spacing of the electrodes will also determine the maximum depth of the material that affects the resistivity reading. If the spacing is too large relative to the size of the member, boundary effects will play a role and the reading obtained will not be a good approximation.

The 4" x 8" cylinders were prepared in accordance with ASTM C 192 and tested with a surface resistivity meter using a Wenner linear four probe array. The Wenner probe array spacing was a fixed spacing of 2.0". The intent of this test was to compare a ternary mixture to a mixture design of concrete made entirely of Type II/V cement with no supplementary cementitious materials added. ASTM C1202 is the Rapid Chloride Permeability Test which measures the electrical conductivity of a 50 mm thick specimen over 6 hours. There is an excessive amount of preparation required before testing can even begin. There has recently been considerable focus on trying to develop a better method for modeling the electrical resistivity/conductivity of concrete to be tested. Resistivity/conductivity of concrete can be used to assist in estimating service life of concrete structures. Agencies have been moving toward performance-based specifications in order to achieve long life structures. Chloride diffusivity is a property that agencies can specify to help ensure a more durable concrete structure. The current ASTM C1202 or AASHTO T 277 are time consuming and cumbersome. Resistivity

measurements can give rapid results and become a helpful tool that will help owners and engineers estimate the useful life of existing and new structures.

Specimens were moist cured continuously until the time of testing. Three identical specimens were prepared in accordance with ASTM C192. Specimens were marked at 90° intervals to serve as a visual guide when taking surface resistivity readings. The sponges on the ends of the Wenner probe were placed longitudinally along the side of the specimen at the first mark with all points making good contact with the specimen. Readings were recorded after the reading had stabilized. Resistivity measurements were taken at 7, 28, and 58 days by placing the resistivity meter on the cylinder at 90° intervals around the cylinder twice. The resistivity of the specimen was calculated as the average of the eight readings.

Table 5 Chemical composition of Type I/II Cement and SCM

Chemical (%)	Type I/II Cement	Chemical (%)	GGBFS 120	Class F Fly Ash
CaO	64.0	CaO	36.77	3.78
SiO <sub>2</sub>	20.4	SiO <sub>2</sub>	36.81	45.05
Al <sub>2</sub> O <sub>3</sub>	3.6	Al <sub>2</sub> O <sub>3</sub>	9.66	23.71
Fe <sub>2</sub> O <sub>3</sub>	3.7	Fe <sub>2</sub> O <sub>3</sub>	0.61	16.43
MgO	2.1	MgO	10.03	0.88
K <sub>2</sub> O	0.69	K <sub>2</sub> O	0.35	1.46
Na <sub>2</sub> O	0.04	Na <sub>2</sub> O	0.31	0.80
SO <sub>3</sub>	2.7	SO <sub>3</sub>	----	0.68
CaCO <sub>3</sub> (in Limestone)	97.0	P <sub>2</sub> O <sub>5</sub>	0.01	0.24
Limestone	6.0	TiO <sub>2</sub>	0.49	1.15
C <sub>3</sub> S	61.2	SrO	0.05	0.18
C <sub>2</sub> S	12.2	Mn <sub>2</sub> O <sub>3</sub>	0.39	0.03
C <sub>3</sub> A	3.3	LOI	----	5.39
C <sub>4</sub> AF	11.2	BaO	----	0.10
C <sub>4</sub> AF+2(C <sub>3</sub> A)	1.10	S	1.10	----



Table 6 Mixture proportions

	Mixture 1	Mixture 2
Coarse Aggregate	1813 lbs/yd <sup>3</sup>	1813 lbs/yd <sup>3</sup>
Fine Aggregate	1225 lbs/yd <sup>3</sup>	1187 lbs/yd <sup>3</sup>
Type I/II Cement	564 lbs/yd <sup>3</sup>	338 lbs/yd <sup>3</sup>
Class F Fly Ash	0	113 lbs/yd <sup>3</sup>
GGBFS	0	113 lbs/yd <sup>3</sup>
Air Entrainer	100 mL/ yd <sup>3</sup>	100 mL/ yd <sup>3</sup>
HRWR	1500 mL/ yd <sup>3</sup>	1100 mL/ yd <sup>3</sup>
Water	263 lbs/yd <sup>3</sup>	263 lbs/yd <sup>3</sup>

Table 7 Chemical composition of steel

	Black	Duplex	Clad
C	0.3	0.02	0.021
Si	0.26	1.0	0.44
Mn	1.22	2.00	1.39
P	0.013	0.035	0.036
S	0.032	0.015	0.006
N	--	0.17	0.034
Cr	0.21	22.0	17.11
Cu	--	0.6	--
Mo	0.04	3.1	2.02
Ni	0.19	4.8	10.02



Figure 6 Undamaged ECR bars



Figure 7 ECR end cut

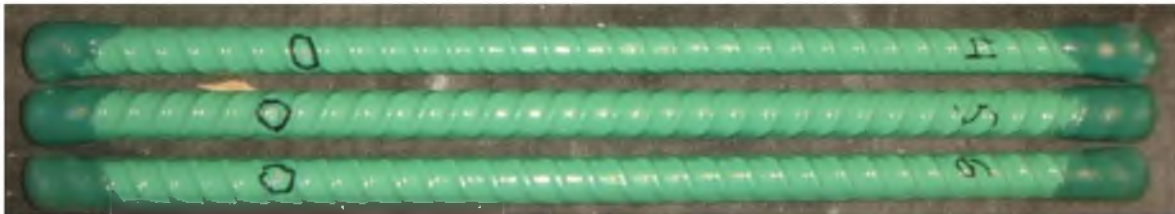


Figure 8 ECR with pinhole damage



Figure 9 ECR bars with "mash" damage



Figure 10 Duplex bars as-received

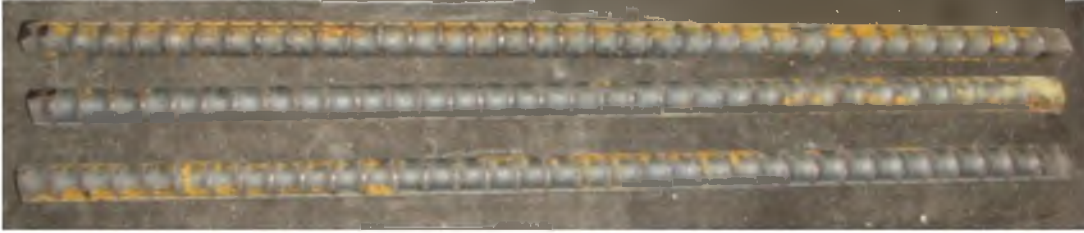


Figure 11 Black bars as-received



Figure 12 SSC end cut



Figure 13 ECR and SSC pin-hole

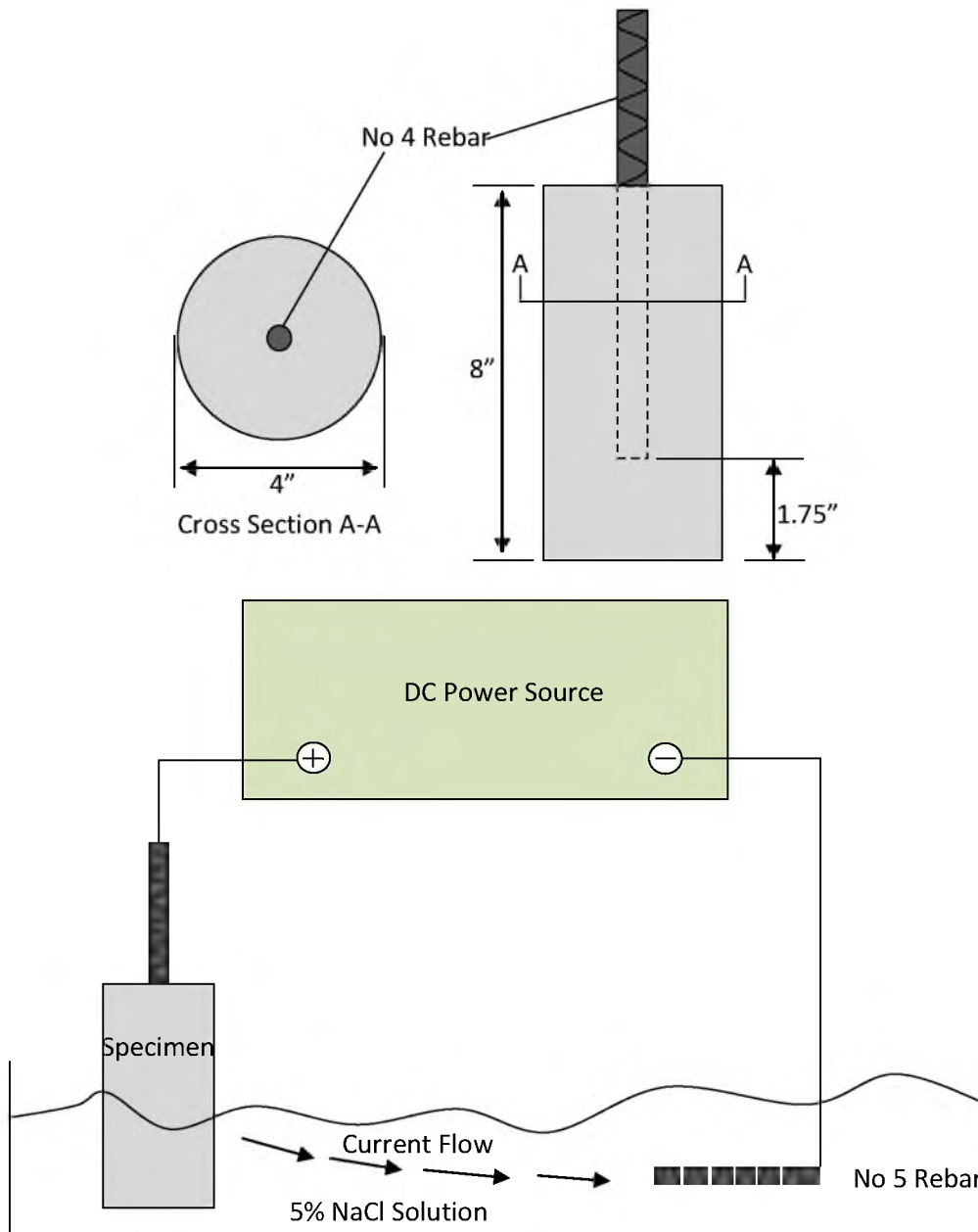


Figure 14 Test schematic for impressed current test (Florida DOT, 2004)

Table 8 Probability of corrosion according to a copper copper-sulfate half cell (ASTM C-876)

Half cell Potential	Corrosion Activity
Less than -200 mV	90% probability of no corrosion
Between -200 and -350 mV	Uncertain corrosion activity
More negative than -350 mV	90% probability of corrosion activity

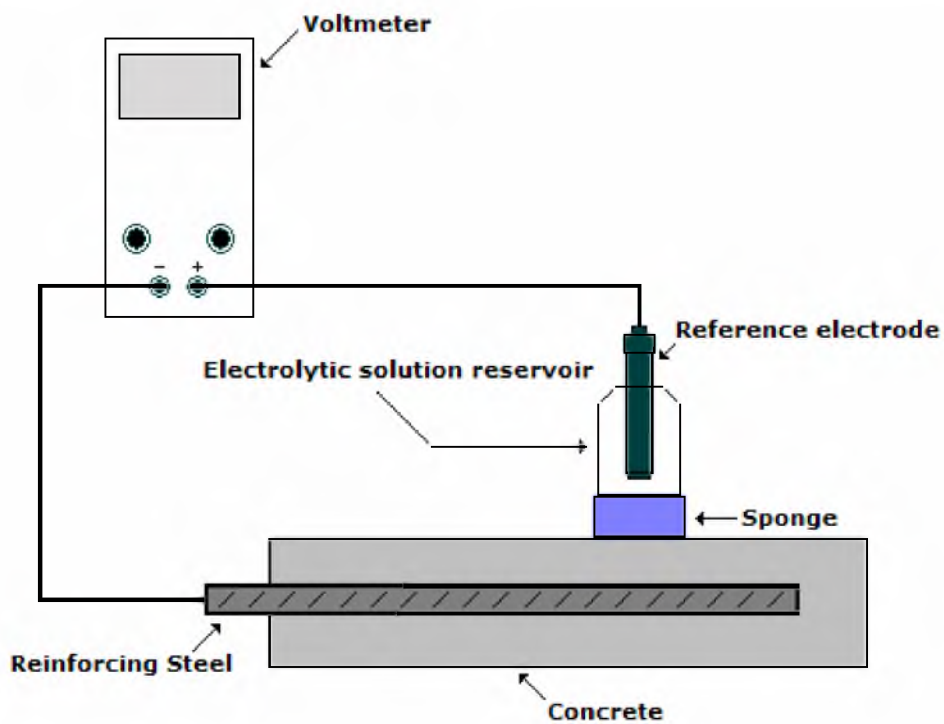


Figure 15 Test schematic for half cell potential test (Guthrie, 2008)

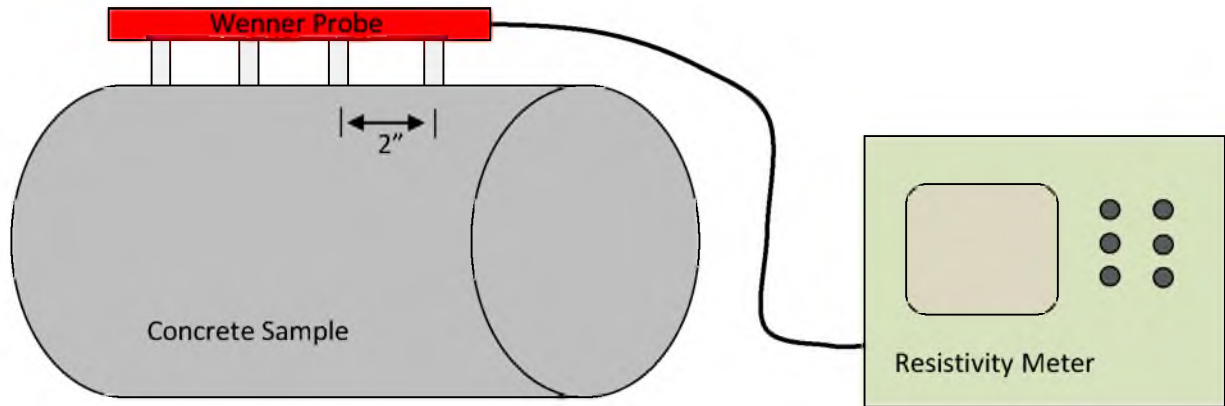


Figure 16 Test schematic for resistivity test

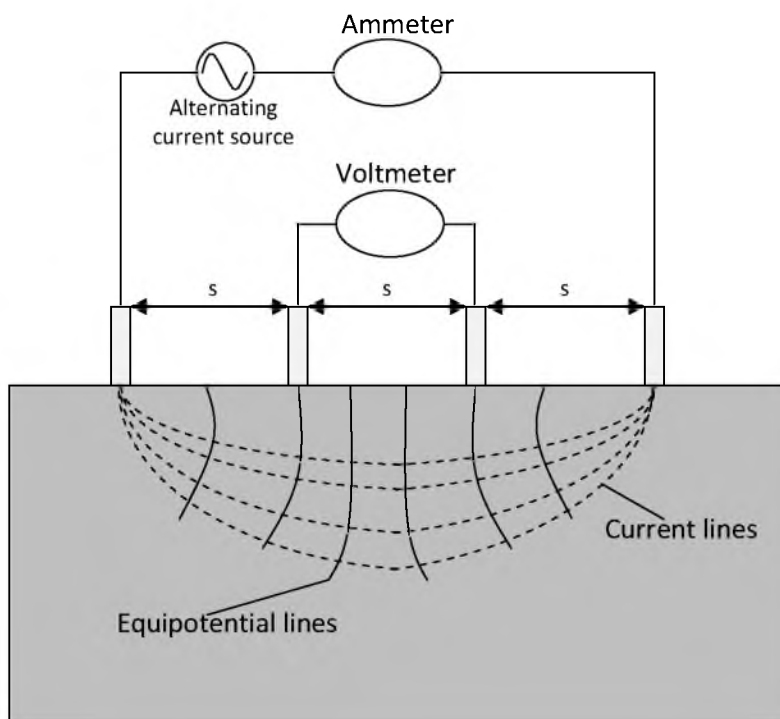


Figure 17 Four probe resistivity schematic

## CHAPTER 4

### RESULTS

The initial time for the impressed current was taken as the time that current was impressed into the specimen. The time to failure was said to be when a crack was detectable by visual means or when there was a large increase in current.

#### 4.1 Impressed Current

The stainless steel clad bars had the shortest time to failure. The duplex bars failed next followed by the black bars. The epoxy coated bars in the pinhole condition and the mashed condition showed no signs of corrosion. The end cut epoxy bars showed signs of corrosion at the damaged site of the epoxy bar. The type I/II concrete mixture specimens corroded faster than their ternary mixture counterparts.

The graph shown in Figure 21 at the end of this chapter shows the current vs time of the black bars cast into the OPC mixtures. Two out of the three black bars in the OPC mixture failed during the test period. There is a jump in the current at the failure time of around 40 and 42 days of testing. Figure 22 and Figure 23 show the specimens after failure and corrosion products are visible. The third specimen did not fail during the period.

Figure 24 is the graph of the current vs time of the black bars cast into the ternary mixtures. None of the black bars in the ternary mixture failed during the test

period. There is no jump in the current readings throughout the test period. Figure 25 and Figure 26 show the specimens after failure and no corrosion products are visible. Figure 27 shows a visual comparison of the corrosion protection offered by specifying a ternary concrete mixture over that of mixture containing only ordinary portland cement.

The graph shown in Figure 28 shows the current vs time of the mid-chromium stainless bars cast into the OPC mixtures. All three of the mid-chromium stainless bars in the OPC mixture failed during the test period. There is an observable jump in the current at the failure time of around 19 and 20 days of testing. Figure 29 shows one of the specimens after failure and corrosion products are visible. There is severe corrosion visible. Figure 30 shows a visual comparison of black bars cast into OPC cylinders versus stainless bars cast into OPC.

Figure 31 is the graph of the current vs time of the mid-chromium stainless bars cast into the ternary mixtures. Current readings during the testing period produced sporadic results. None of the mid-chromium stainless bars in the ternary mixture failed during the test period. No corrosion products were visible when the specimens were cracked open. Figure 32 shows a visual comparison of the corrosion protection offered by specifying a ternary concrete mixture over that of mixture containing only ordinary portland cement.

Figure 33 shows the current vs time of the stainless steel clad bars as-received cast into the OPC mixtures. All three of the stainless steel clad bars in the OPC mixture failed during the test period. There is an observable jump in the current at the failure time of around 19 and 20 days of testing. Figure 34 shows one of the specimens after failure and corrosion products are visible. There is severe corrosion visible.



Figure 35 shows the current vs time of the stainless steel clad bars pinhole condition cast into the OPC mixtures. All three of the bars failed during the test period. There is an observable jump in the current vs time graph at the failure time of around 12 and 20 days of testing. There was severe corrosion visible at the end of the test as seen in Figure 36. Both the as-received condition and the pinhole condition for the SSC bars in an OPC mixture performed similarly during the impressed current test.

Figure 37 shows the current vs time of the stainless steel clad bars as-received cast into the ternary mixtures. None of the three stainless steel clad bars in the ternary mixture failed during the test period. Figures 38 and 39 show the three specimens after failure and corrosion products are visible but the cylinders did not crack during the test period. Figure 40 shows a visual comparison of black bars cast into OPC cylinders versus stainless bars cast into OPC.

Figure 41 shows the current vs time of the epoxy coated bars mash condition cast into the OPC mixtures. The current vs time graph remains low and steady throughout the duration of the test. None of the bars failed during the test period. Figure 42 shows one of the specimens at the end of the test and no corrosion products are visible.

Figure 43 shows the current vs time of the epoxy coated bars pinhole condition cast into the OPC mixtures. None of the bars failed during the test period. Figure 44 shows one of the specimens at the end of the test and no corrosion products are visible.

Figure 45 shows the current vs time of the epoxy coated bars endcut condition cast into the OPC mixtures. None of the bars failed during the test period. Figure 46 shows one of the specimens at the end of the test and there are corrosion products visible; however, the specimens did not crack during the test period.

Figure 47 shows the current vs time of the epoxy coated bars endcut condition cast into the ternary mixtures. None of the bars failed during the test period. Figure 48 shows one of the specimens at the end of the test and there are corrosion products visible; however, the specimens did not crack during the test period.

#### 4.2 Half Cell Potential

The half cell measurements were conducted on the specimens after the cylinders were cast, while the cylinders cured, and throughout the impressed current test. No measurements are reported for the epoxy coated bars as ASTM C876 is not applicable for epoxy coated bars. ASTM C876 states the probability of corrosion based on the results of a Copper/Copper-Sulfate half cell. The values and the corresponding probabilities of corrosion are reported in Table 8.

Figure 49 shows all of the bars and their corresponding half cell potential readings versus time. The ternary specimens all have a lower initial half cell reading but tend to decrease at a slower rate. The black bars also seem to have a lower initial reading.

A comparison of all the types of bars investigated cast into the OPC mixture is shown in Figure 50. The black bars have a lower initial reading than the stainless and the clad bars. The clad bars and the black bars half cell potential readings decrease at roughly the same point. The stainless bars half cell readings decrease at a later time during the experiment.

Figure 51 shows a comparison of all the types of bars investigated cast into the ternary mixture. All of the specimens have a low initial half cell reading. The black bars half cell potential reading is initially lower than the clad and the stainless bars. All of the bars decrease at roughly the same time and decrease at roughly the same rate.

Figure 52 shows a comparison of the black bars cast in ternary and OPC mixtures. All of the specimens have a low initial half cell reading. The black bars cast in the ternary mixture half cell potential reading are initially lower than the OPC counterparts. The ternary bars decrease at a slightly slower rate.

Figure 53 shows a comparison of the stainless bars cast in ternary and OPC mixtures. All of the specimens have a low initial half cell reading. The stainless bars cast in the ternary mixture half cell potential reading are initially lower than the OPC counterparts. The ternary bars decrease at roughly the same rate.

Figure 54 shows a comparison of the clad bars cast in ternary and OPC mixtures. The black bars cast in the ternary mixture half cell potential reading are initially lower than the OPC counterparts. The ternary bars decrease at a slightly slower rate.

### 4.3 Resistivity

A plot of the resistance vs time of the two mixtures investigated is shown in Figure 55. The ternary mixture has a lower initial resistance but quickly reaches a much higher resistance than the ordinary portland cement mixture. The ternary mixture had higher resistivity than mixtures that used only portland cement.

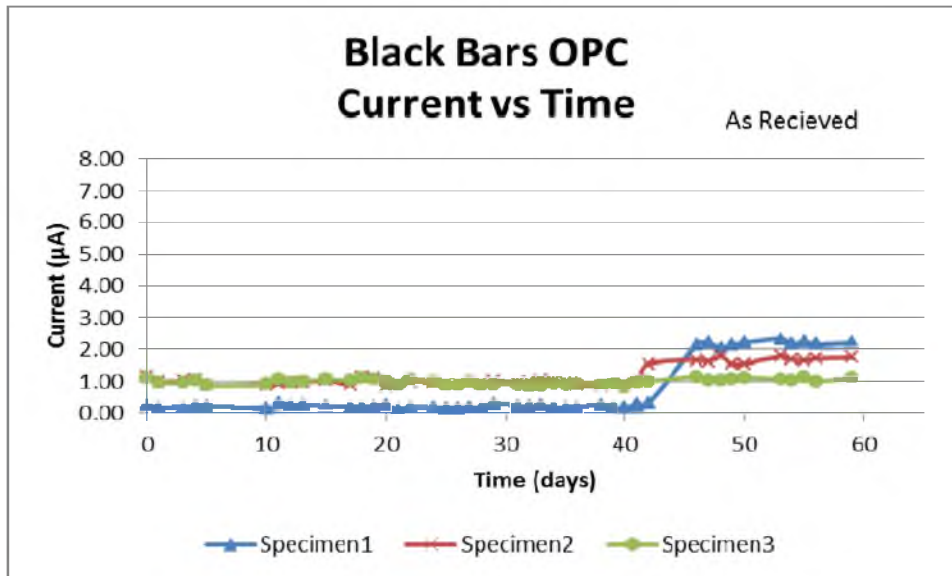


Figure 18 Black bars in OPC current vs time



Figure 19 Black bar in OPC after impressed current test



Figure 20 Black bar in OPC after impressed current test

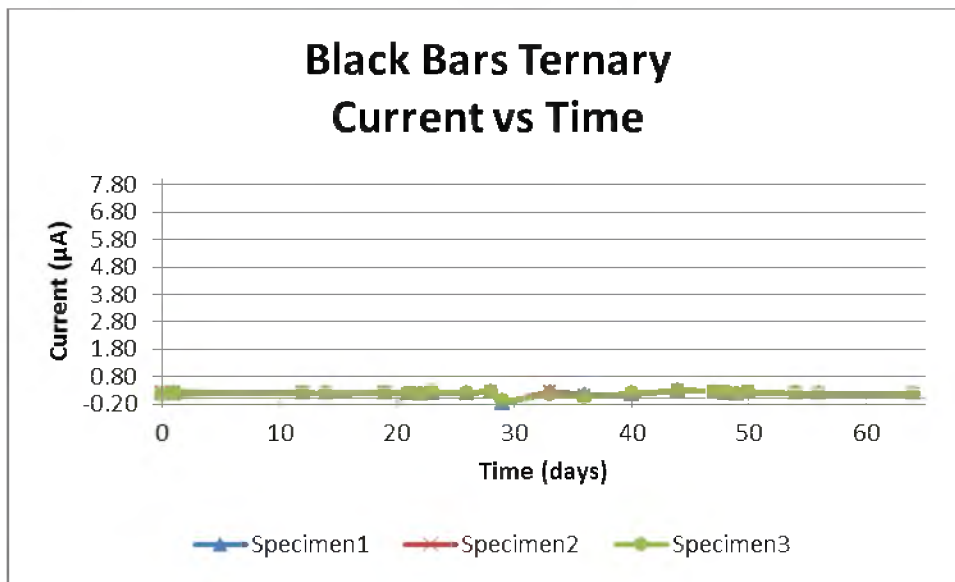


Figure 21 Black bars in ternary current vs time

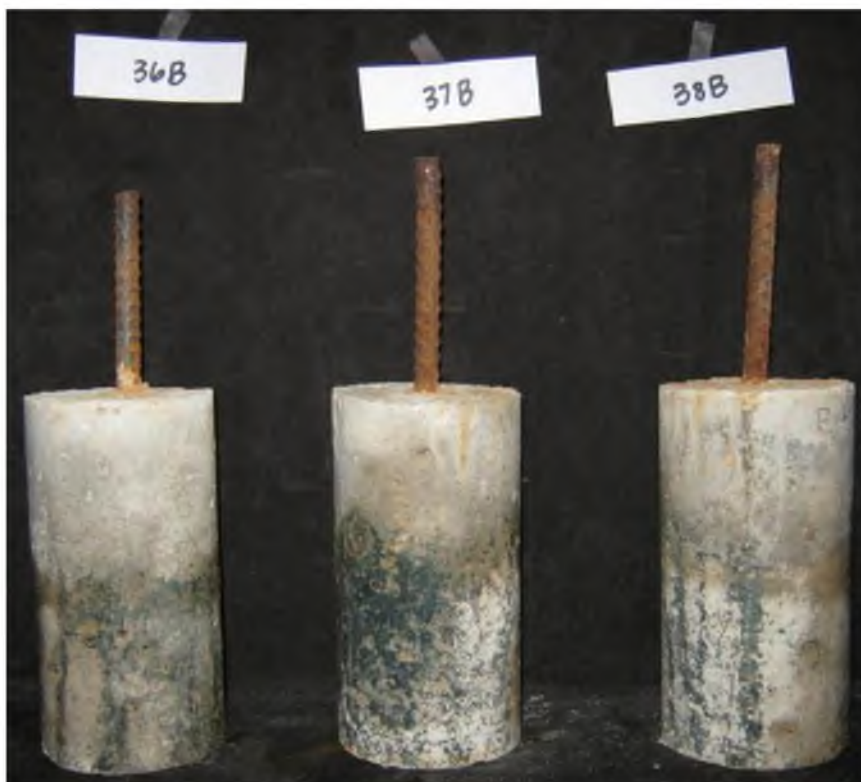


Figure 22 Black bars in ternary after impressed current test



Figure 23 Black bars in ternary after impressed current test



Figure 24 Visual comparison of ternary vs OPC specimens containing black bars

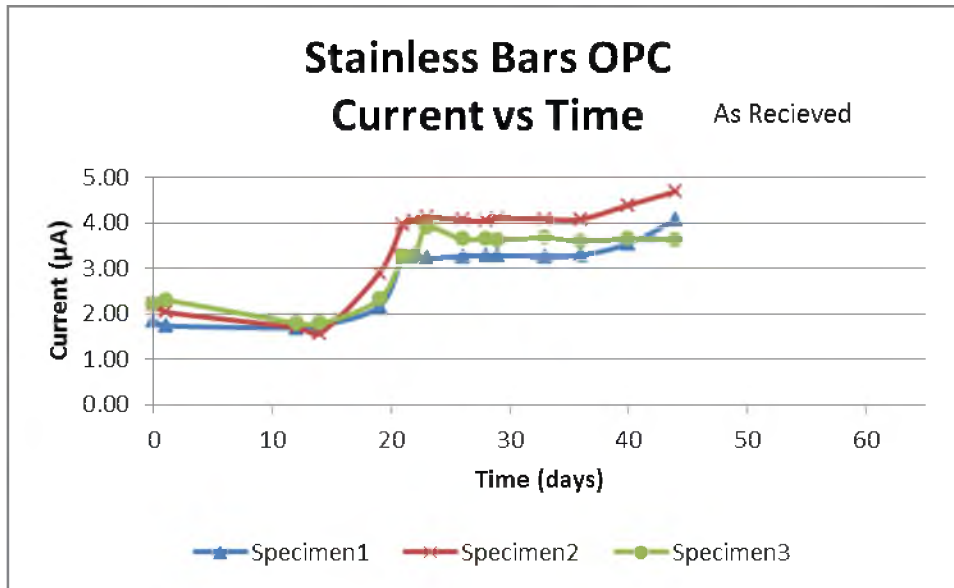


Figure 25 Stainless bars in OPC current vs time



Figure 26 SSA in OPC after impressed current test





Figure 27 Visual comparison of SSA and black bars in OPC

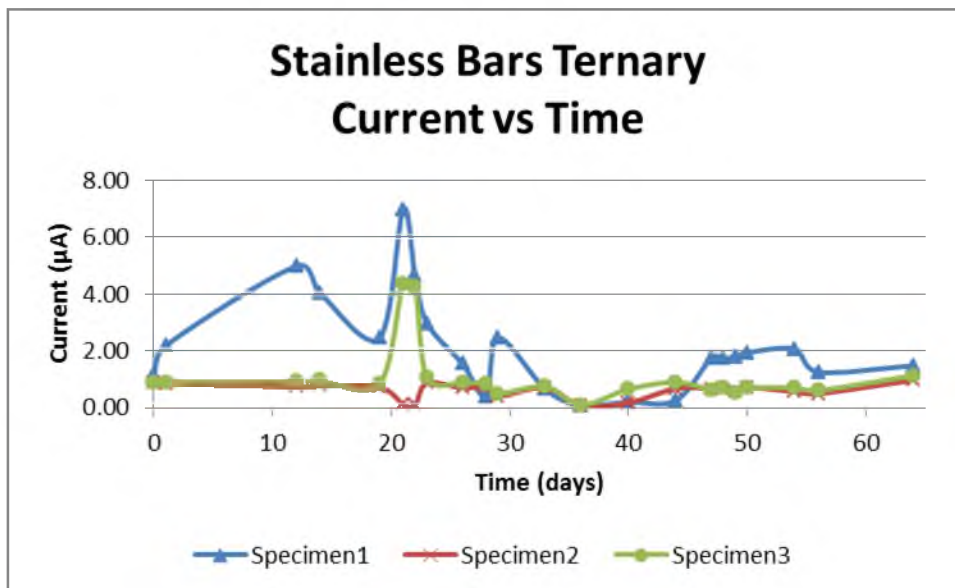


Figure 28 Stainless bars in ternary current vs time



Figure 29 Visual comparison of OPC and ternary SSA bars

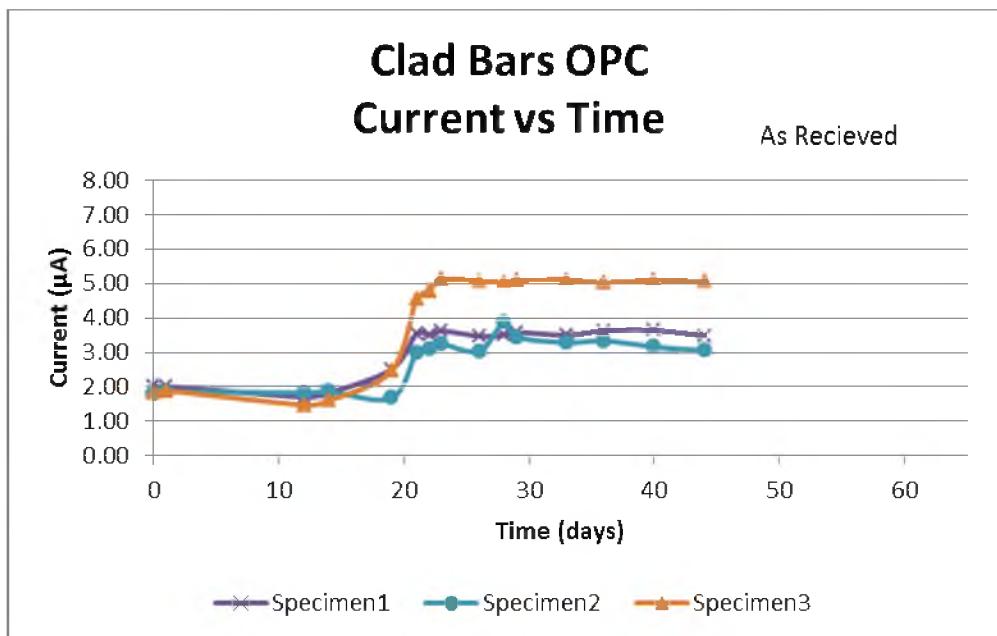


Figure 30 Clad bars in OPC as-received current vs time



Figure 31 OPC SSC bars (as-received) after impressed current test

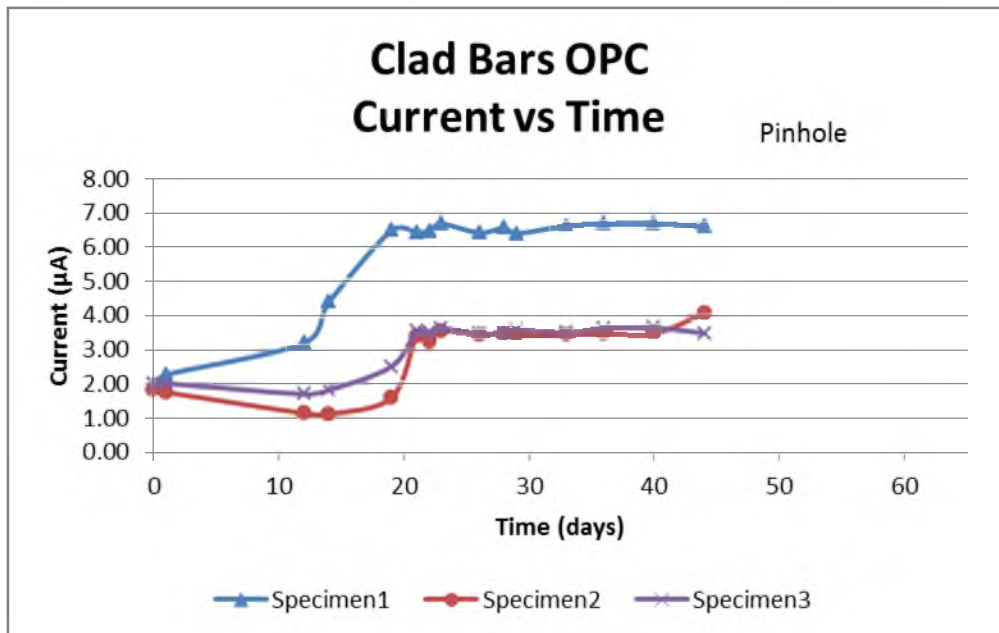


Figure 32 Clad bars in OPC pinhole current vs time



Figure 33 SSC bar (pinhole) in OPC after impressed current test

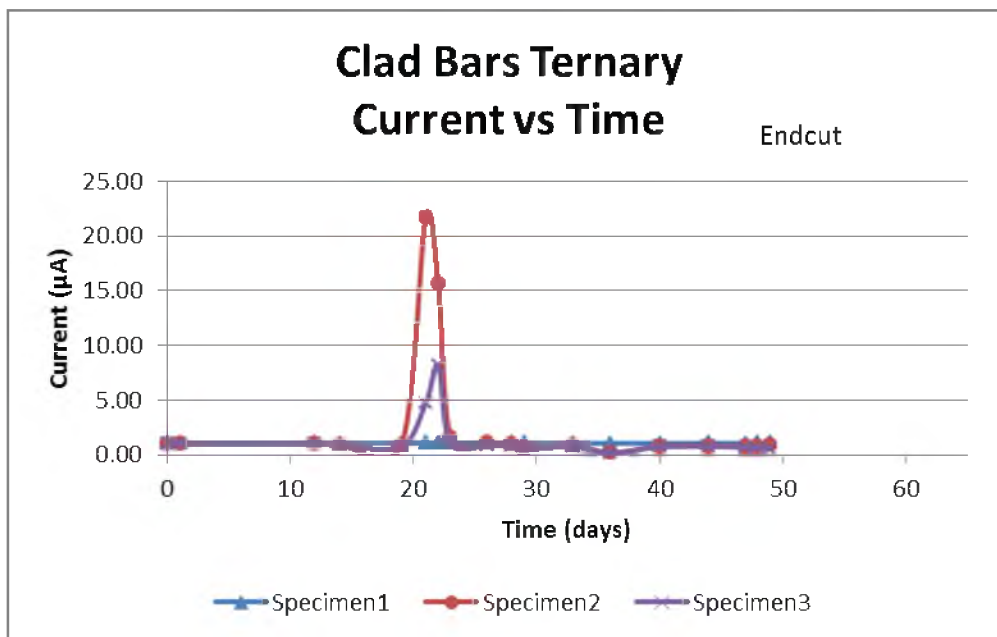


Figure 34 Clad bars in ternary endcut current vs time



Figure 35 Ternary SSC (end cut) after impressed current test



Figure 36 SSC bar in ternary (end cut) after impressed current test



Figure 37 Comparison of OPC and ternary SSC bars

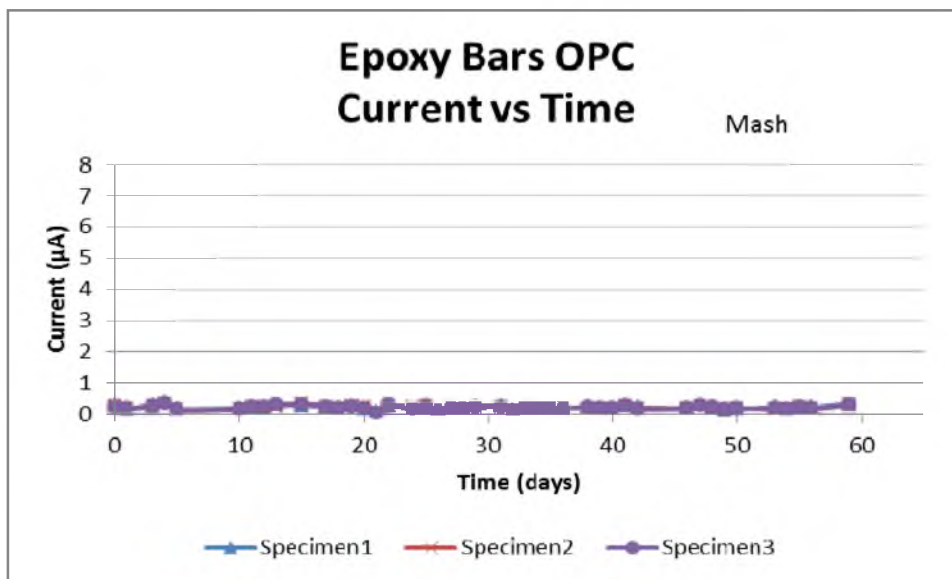


Figure 38 Epoxy bars in OPC mash current vs time



Figure 39 ECR (mashed) in OPC after impressed current test

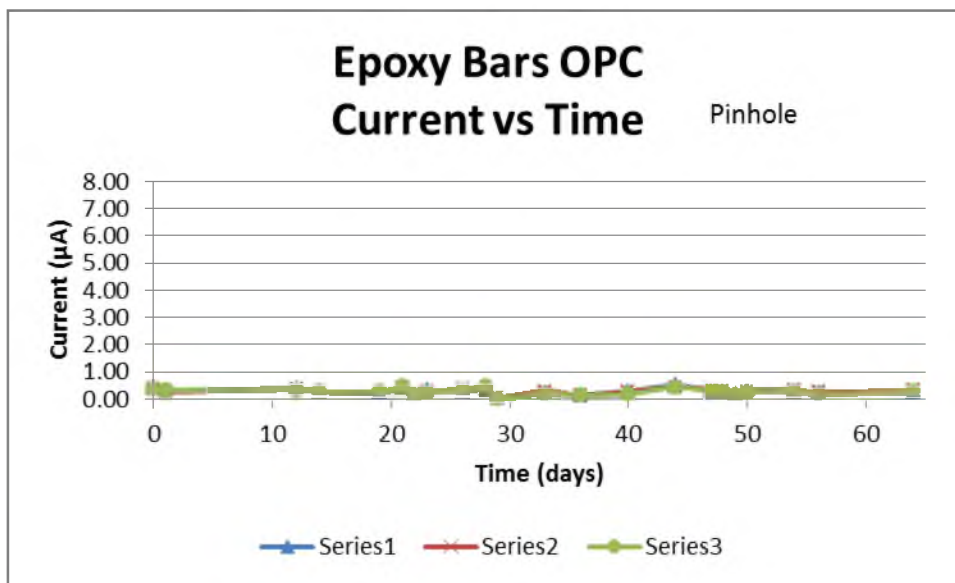


Figure 40 Epoxy bars in OPC pinhole current vs time



Figure 41 ECR (pinhole) in OPC after impressed current test

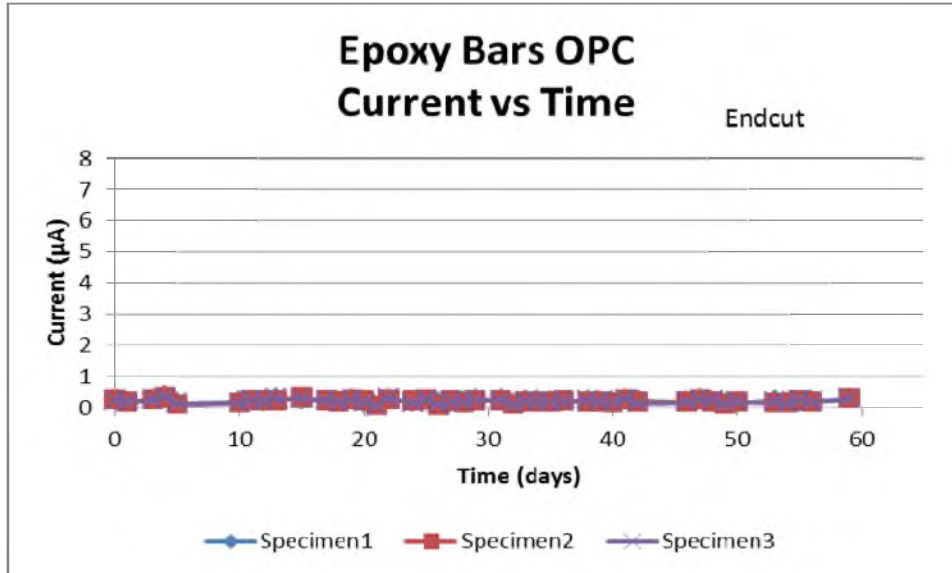


Figure 42 Epoxy bars in OPC endcut current vs time



Figure 43 ECR (endcut) in OPC after impressed current test



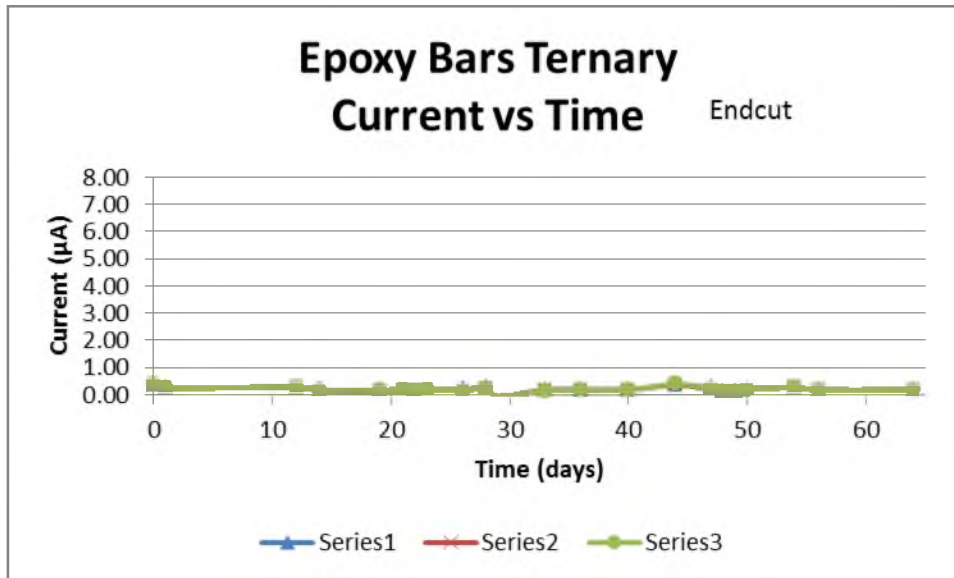


Figure 44 Epoxy bars in ternary endcut current vs time



Figure 45 ECR (endcut) in ternary after impressed current test

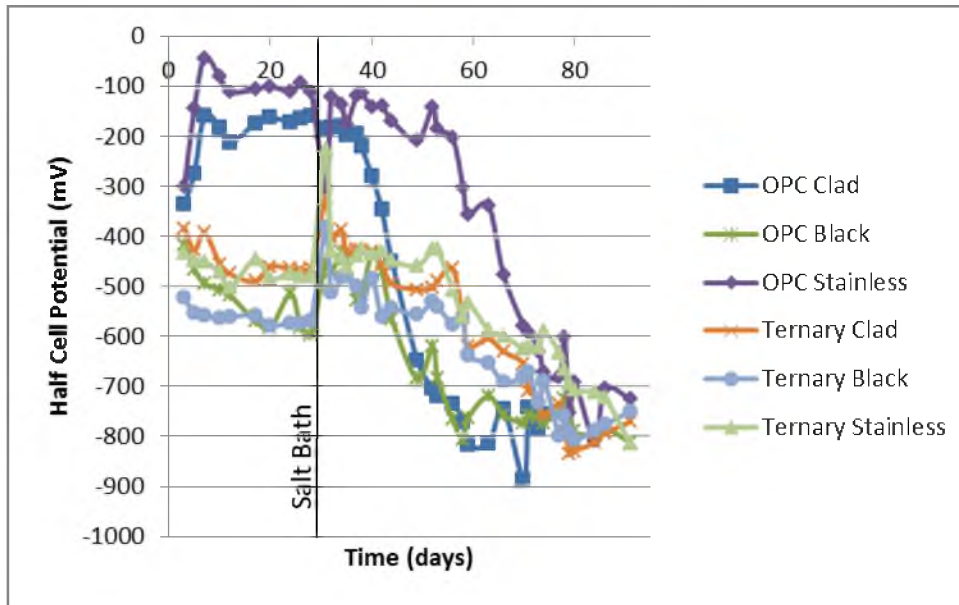


Figure 46 Half cell potential vs time for all the specimens studied

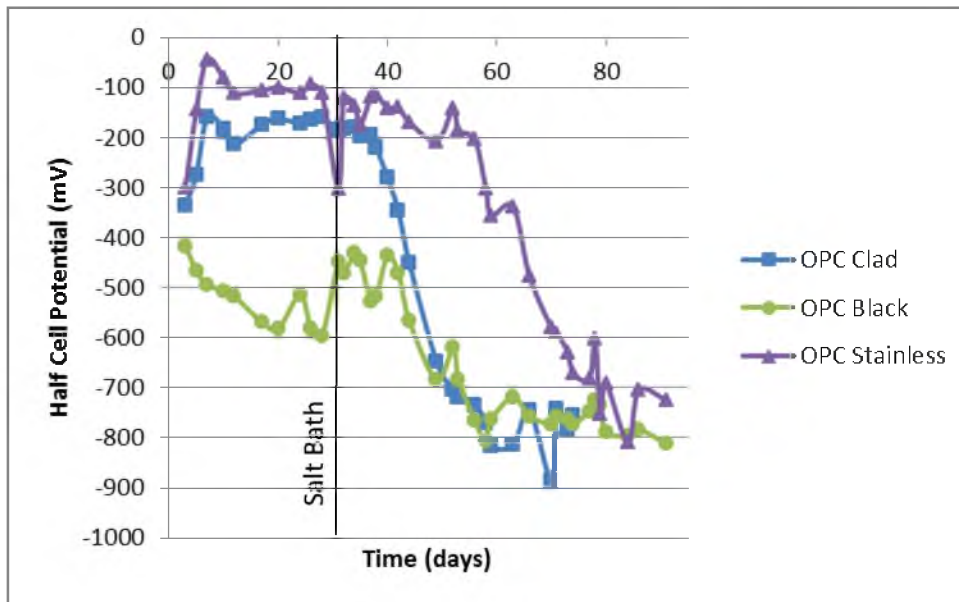


Figure 47 Comparison of half cell potential of different bars (as-received) in OPC

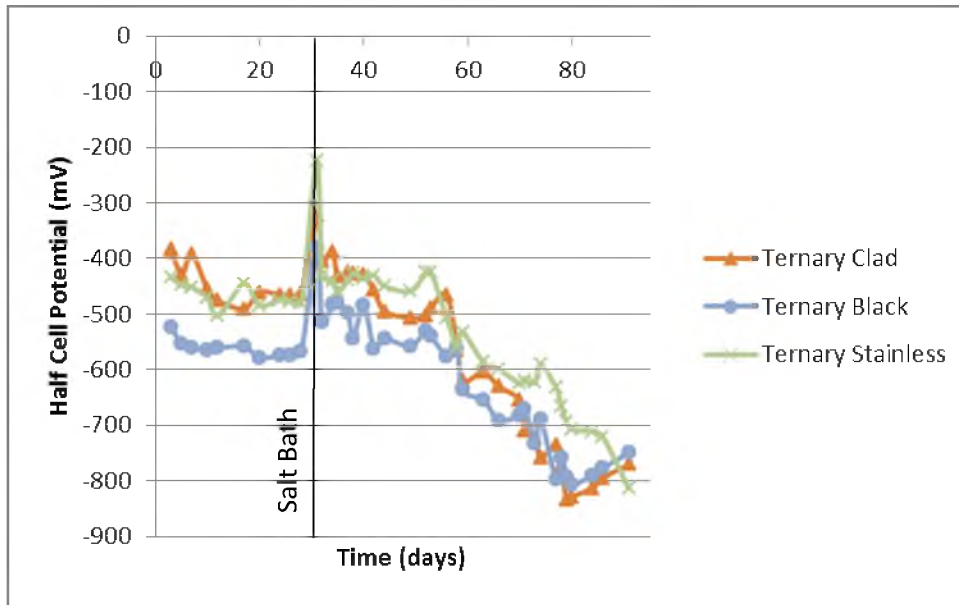


Figure 48 Comparison of half cell potential of different bars (as-received) in ternary

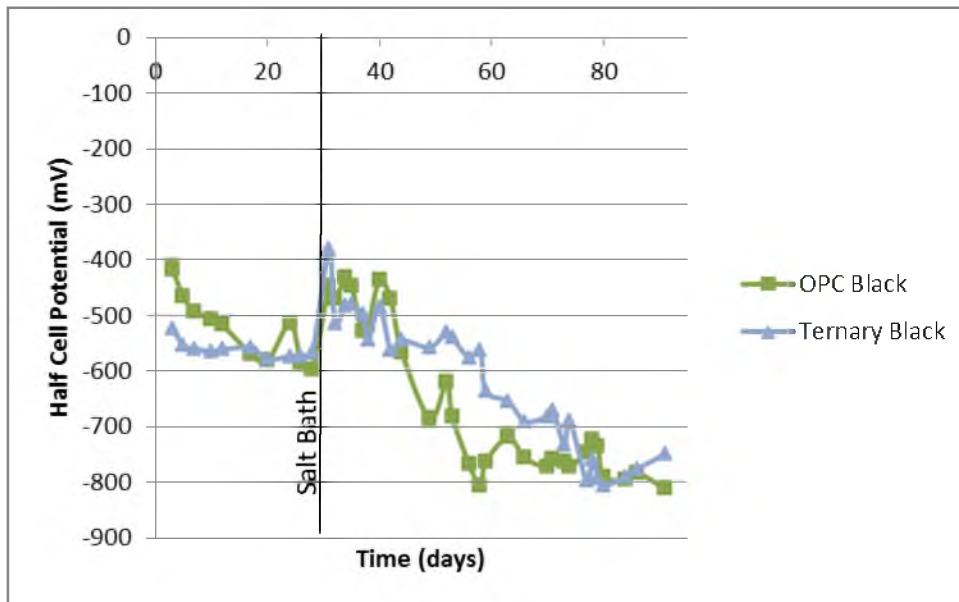


Figure 49 OPC and ternary comparison of half cell potential of black bars

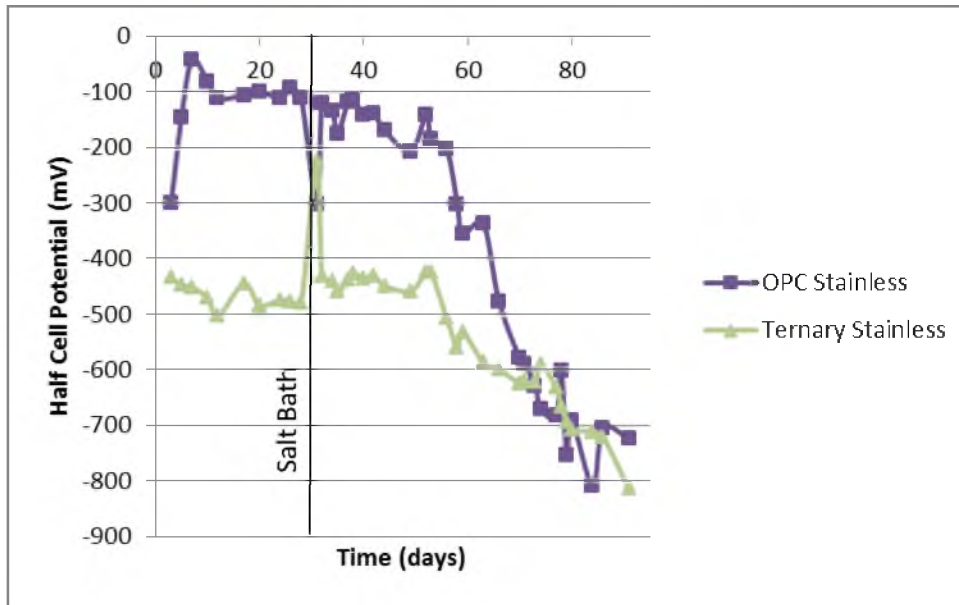


Figure 50 OPC and ternary comparison of half cell potential of SSA bars

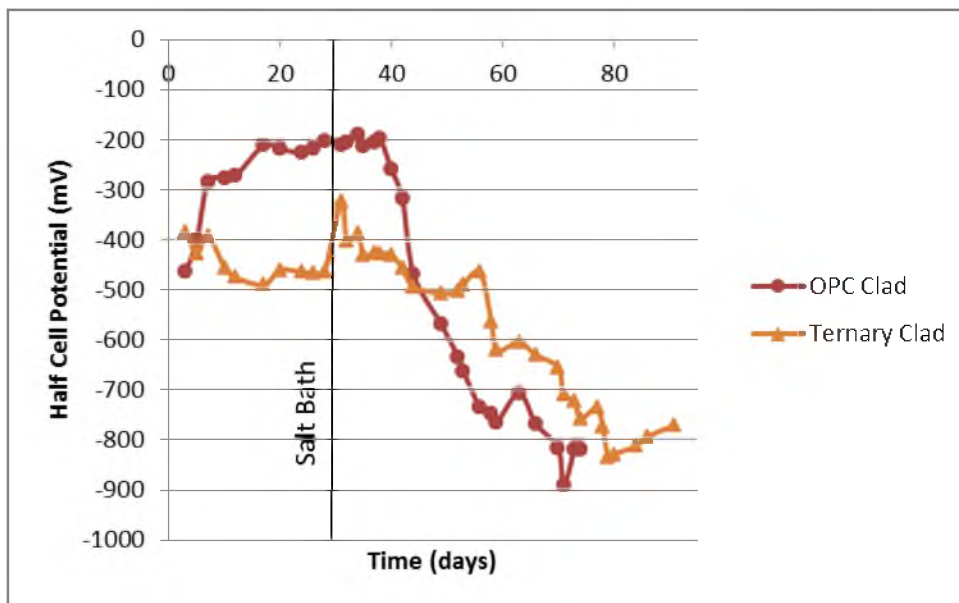


Figure 51 OPC and ternary comparison of half cell potential of SSC bars (endcut)

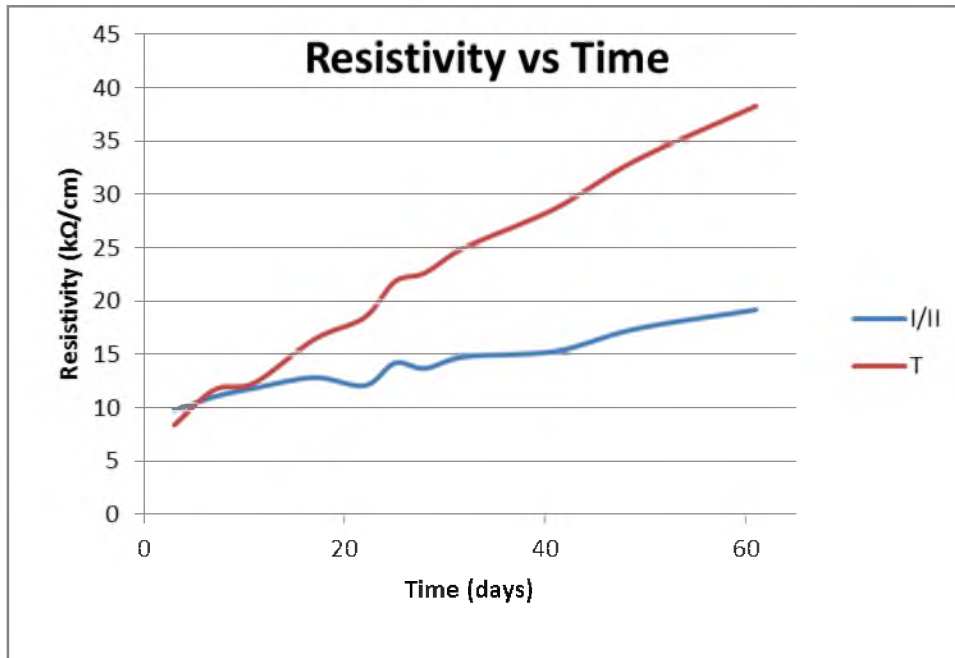


Figure 52- Resistance vs time comparison of OPC and ternary

## CHAPTER 5

### CONCLUSIONS

The data suggest that even improperly handled and placed epoxy coated rebar are the superior choice for designers looking to achieve 100-year life cycles. The ternary mixtures yielded better test results for all of the steel tested. However, the half cell potential test of the ternary mixtures produced misleading results, suggesting a high probability of corrosion (see Table 8) from the beginning of the test period. This is most likely due to the higher concentration of alkalis in the GGBFS supplementary cementitious material used.

The data also suggest that black bars, with proper coverage and the right concrete mixture, can produce long life structures even under high demand conditions. The black bars did not perform well in the OPC mixtures made with Type I/II cement, but performed surprisingly well in the ternary concrete mixture. Black bars represent the lowest initial cost for reinforcement, but could end up having very high repair costs over the anticipated life of the structure if the right concrete mixture and cover are not properly specified by the designer and built by the contractor.

The stainless steel clad bars did not perform well with either concrete mixture. The specimens showed pitting and heavy section loss when cast in the OPC mixtures. The SSC specimens cast in the ternary mixture began to show signs of deterioration

intended use and the exposure conditions for concrete structures containing stainless steel clad bars.

The mid-chromium stainless steel bars also did not perform well in the impressed current test. Some of the specimens showed more severe deterioration than their black bar counterparts. Long life structures may still be achievable reinforced with a mid-chromium stainless steel provided other corrosion preventative measures are taken. Designers and contractors should use caution when specifying mid-chromium stainless steel bars.

The epoxy coated bars showed the best performance for the tests performed. Even with pinholes and meshes, the epoxy coated bars showed no signs of corrosion. The endcut condition showed signs of corrosion after the test period. As long as the contractor repairs any cut ends per the manufacturer's recommendations, concrete reinforced with epoxy coated bars should yield the longest life structures of the bars investigated regardless of the permeability of the concrete mixture used. However, using a low-permeability concrete with proper cover will add extra protection should there be an issue with the protective coating.

In order to achieve the proper design life, the author recommends that designers explicitly and concisely specify proper materials and procedures for the exposure conditions of the structure. It is also recommended that strict quality assurance measures be implemented to ensure that the owner is receiving the structure with the design life that the designer has designed. Using proper materials and procedures designers and contractors can build long life structures that will meet and exceed the increasing

engineering demands of harsh exposure conditions and save the owner money over the life of the structure compared to if initial cost saving materials or procedures were used.



## REFERENCES

- Abu, K. (2003). *Evaluation of MMFX Corrosion Resistant Steel Dowel Bars in Concrete Pavements*. Wisconsin Department of Transportation.
- Aly, R., Benmokrane, B., & Ebead, U. (2006). Tensile Lap Splicing of Fiber-Reinforced Polymer Reinforcing Bars in Concrete. *ACI Structural Journal*.
- American Concrete Institute. (2007). *Manual of Concrete Practice*. Farmington Hills, MI.
- Berg, A. C., Bank, L. C., Oliva, M. G., & Russell, J. S. (2006). Construction and Cost Analysis of an FRP Reinforced Concrete Bridge Deck. *Construction and Building Materials*, 20.
- Brown, M. C., Weyers, R. E., & Via, C. E. (2003). *Corrosion Protection Service Life of Epoxy Coated Reinforcing Steel in Virginia Bridge Decks*. Virginia Transportation Research Council.
- Chowdhury, P. C. (2004). Strategies for Resisting Corrosion of Reinforcement in Concrete. *The Indian Concrete Journal*.
- Clausen, K. A. (2004). Striving for Durable Bridge Decks with Life-365 and the Control of Cracking.
- Clemena, G. G. (2003). *Investigation of the Resistance of Several New Metallic Reinforcing Bars to Chloride- Induced Corrosion in Concrete*. Virginia Transportation Research Council.
- Clemena, G. G. (2004). *Resistance of a Stainless Steel Clad Reinforcing Bar to Chloride Induced Corrosion in Concrete*. Virginia Transportation Research Council.
- Cross, W. M., Duke, E. F., Kellar, J. J., Han, K. N., & Johnston, D. (2001). *Stainless Steel Clad Rebar in Bridge Decks*. South Dakota Department of Transportation.
- Cui, F., & Krauss, P. D. (2006). *Corrosion Resistance of Alternative Reinforcing Bars: An Accelerated Test*. CRSI.
- Darwin, D., Browning, J., Gong, L., & Hughes, S. R. (2007). *Effects of Deicers on Concrete Deterioration*. The University of Kansas Center for Research.
- Darwin, D., Browning, J., Locke, C. E., & Nguyen, T. V. (2007). *Multiple Corrosion Protection Systems for Reinforced Concrete Bridge Components*. Federal Highway

Administration.

Darwin, D., Browning, J., Nguyen, T. V., & Locke, C. J. (2002). *Mechanical and Corrosion Properties of High Strength, High Chromium Reinforcing Steel for Concrete*.

Dietsche, J. S. (2002). *Development of Material Specifications for FRP Structural Elements for the Reinforcing of a Concrete Bridge Deck*. University of Wisconsin-Madison.

Environmental Effects on the Mechanical Properties of E-Glass FRP Rebars. (1998). *ACI Materials Journal* (March- April).

Gong, L., Darwin, D., Browning, J. P., & Locke, C. E. (2002). *Evaluation of Mechanical and Corrosion Properties of MMFX Reinforcing Steel for Concrete*. South Dakota Department of Transportation.

Guthrie, W. S., Pinkerton, T. M., Eggett, D. L. (2008) *Sensitivity of Half- Cell Potential Measurements to Properties of Concrete Bridge Decks*. Utah Department of Transportation.

Hartt, W. H., Powers, R. G., Leroux, V., & Lysogorski, D. K. (2004). *A Critical Literature Review of High Performance Corrosion Reinforcements in Concrete Bridge Applications*. Federal Highway Administration.

Hartt, W. H., Powers, R. G., Lysogorski, D. K., Liroux, V., & Virmani, Y. P. (2007). *Corrosion Resistant Alloys for Reinforced Concrete*. Federal Highway Administration.

Hartt, W. H., Powers, R. G., Lysogorski, D. K., Paredes, M., & Virmani, Y. P. (2006). *Job Site Evaluation of Corrosion Resistant Alloys for Use as Reinforcement in Concrete*. Federal Highway Administration.

Hartt, W., Lysogorski, D., & Leroux, V. (2004). Characterization of Corrosion Resistant Reinforcement by Accelerated Testing. *CBC* .

High Performance Concrete Technology Delivery Team. (2005). *High Performance Concrete Structural Designers' Guide*. Federal Highway Administration.

Humphreys, S. R. (2004). Improving the Quality of Epoxy Coated Steel Reinforcing Bars through CRSI's Epoxy Coating Applicator Certification Program. *CBC* .

Jolley, M. J., Fanous, F., Phares, B., & Wipf, T. J. (2005). *Evaluation of Corrosion Resistance of Different Steel Reinforcement Types*. Transportation Research Board.

Kahl, S. (2007). *Corrosion Resistant Alloy Steel (MMFX) Reinforcing Bar in Bridge Decks*. Michigan Department of Transportation.

- Konecny, P., Tikalsky, P., Tepke, D., (2006) *Performance Assessment of a Concrete Bridge Deck Applying SBRA Approach*, IABSE Symposium on Responding to Tomorrow's Challenges in Structural Engineering, Budapest, Hungary, September, 2006
- Kusinski, G., & Thomas, G. (2005). *High Strength Toughness and Nanostructure Considerations for Fe/Cr/Mn/C Lath Martensitic Steels*. MMFX Technologies Corporation.
- Lee, S.-K., & Krauss, P. D. (2004). *Long Term Performance of Epoxy Coated Reinforcing Steel in Heavy Salt Contaminated Concrete*. Federal Highway Administration.
- Li, C. Q., Yang, Y., & Melchers, R. E. (2008). *Prediction of Reinforcement Corrosion in Concrete and Its Effects on Concrete Cracking and Strength Reduction*. ACI Materials Journal
- Lindquist, W. D., Darwin, D., Browning, J., & Miller, G. G. (2006). Effect of Cracking on Chloride Content in Concrete Bridge Decks. *ACI Structural Journal* .
- Linford, M. S., & Reaveley, L. D. (2004). *A Study of the I-15 Reconstruction Project to Investigate Variables Affecting Bridge Deck Cracking*. Utah Department of Transportation.
- Maholtra, V. M., Carino, N. J. (2004) *Handbook on Nondestructive Testing of Concrete*. CRC Press, West Conshohocken, PA
- Marquez, S., Hanson, S., & Tikalsky, P. J. (2008). Environmental Advantages of Ternary Cement Combinations. 2nd International Symposium on Ultra High Performance Concrete.
- Miller, G. G., Kepler, J. L., & Darwin, D. (2003). Effect of Epoxy Coating Thickness on Bond Strength of Reinforcing Bars. *ACI Structural Journal* .
- Nanni, A. (2000). FRP Reinforcement for Bridge Structures. Lawrence: Proceedings of the Structural Engineering Conference.
- Nanni, A., & Faza, S. (2002). Designing and Constructing with FRP Bars: An Emerging Technology. *Concrete International* .
- National Cooperative Highway Research Program. (2000). *Cost-Effective Practices for Off-System and Local Interest Bridges*. Washington, DC: Transportation Research Board.
- Seliem, H., Lucier, G., Rizkalla, S., & Zia, P. (2006). Behavior of Concrete Bridge Decks Reinforced with High Strength Steel. *CBC* .
- Stundebeck, C. J. (2007). *Durability of Ternary Blended Cements in Bridge Applications*. PCA Research & Development Information.

Tang, B. M. (2003). FRP Composites Technology Brings Advantages to the American Bridge Building Industry. Cairo, Egypt: 2nd International Workshop on Structural Composites for Infrastructure Applications.

Tepke, D. G., & Tikalsky, P. J. (2007). *Best Construction Practices for Concrete Bridge Decks*. The Commonwealth of Pennsylvania Department of Transportation.

Tepke, D. G., & Tikalsky, P. J. (2007). *Best Engineering Practices Guide for Bridge Deck Durability*. The Commonwealth of Pennsylvania Department of Transportation.

Tikalsky, P., Schaefer, V., Wang, K., Scheetz, B., Rupnow, T., St. Clair, A., et al. (2007). *Development of Performance Properties of Ternary Mixtures: Phase I Final Report*. Washington, DC: Federal Highway Administration.

Tuutti, K., *Corrosion of Steel in Concrete*. Swedish Cement and Concrete Research Institute, S-100 44 Stockholm, 1982.

Val, D. V., & Stewart, M. G. (2000). Life-Cycle Performance of RC Bridges: Probabilistic Approach. *Civil and Infrastructure Engineering*, 15.

Williamson, G., Weyers, R. E., Brown, M. C., & Sprinkel, M. M. (2007). *Bridge Deck Service Life Prediction and Cost*. Virginia Transportation Research Council.

Yeomans, S. R. (1991). *Comparative Studies of Galvanized and Epoxy Coated Steel Reinforcement in Concrete*. Australian Defence Force Academy.

Yeomans, S. R. (2002). Galvanized Reinforcing Steel. *Corrosion Management* (November).

Yeomans, S. R., & Novak, M. P. (1990). *Further Studies of the Comparative Properties and Behaviour of Galvanized and Epoxy Coated Steel Reinforcement*. Australian Defence Force Academy.

Yunovich, M., Thompson, N. G., & Virmani, Y. P. (2004). Corrosion of Highway Bridges; Economic Impact and Life Cycle Cost Analysis. *CBC*.